New Tension-Compression Damage Model for Complex Analysis of Concrete Structures

Jairo A. Paredes[1], Sergio Oller[2] and Alex H. Barbat[3]

Abstract

A new damage model, based on continuum damage mechanics and simulating the opening, closing and reopening of cracks in concrete using only one surface of discontinuity, is proposed in this article. The model complies with the thermodynamics principles of non-reversible, isothermal and adiabatic processes. Two scalar internal variables have been defined: a tensile damage variable d^+ and a compressive damage variable d^-; the threshold of damage is controlled by only one surface of discontinuity and a new parameter that controls the damage variable which should be activated. This new parameter represents the ratio of tensile stress to compressive stress in the damaged material. The continuity of response under complex loads, which is one of the aims of this work, is ensured. An adequate response under different types of loads leads to the conclusion that the proposed model provides a powerful tool to numerically analyze reinforced concrete structures. Validation and illustrative examples are included in the article.

Keywords: Damage model; non-linear analysis; concrete, FEM.

INTRODUCTION

Micro-cracking and sliding between granular particles cause the highly non-linear behavior of concrete (Oller 1988), and it is difficult to represent this behavior through constitutive models. These phenomena can be characterized by the cohesion and the inner friction angle, the softening stress strain curve and the volumetric dilatation (Tao and Phillips 2005). They cause the decrease of the material's elastic modulus and strength. If the material is exposed to alternating tensile-compressive stress states, the opening, closing and reopening of cracks can occur. These phenomena must be adequately represented by constitutive models ensuring continuity of the response to complex loads.

Traditionally, constitutive models for concrete use the fracture mechanics theory (CFM) and the continuum damage mechanics theory (CDM). Classical fracture mechanics gives a basis for simulating the opening and closing of cracks. Hillerborg et al. (1976) describe the mechanical behavior of concrete by developing a non-linear fracture model and using the finite element

[1] National University of Colombia, Manizales Campus, A.A. 127, Colombia. E-mail address: japaredesl@unal.edu.co (Corresponding author)

[2] Civil Engineering School–CIMNE, Technical University of Catalonia. c/ Gran Capitan s/n Ed. C1, Campus Nord, 08034 Barcelona, Spain. sergio.oller@upc.edu

[3] Civil Engineering School–CIMNE Technical University of Catalonia. c/ Gran Capitan s/n Ed. C1, Campus Nord, 08034 Barcelona, Spain. alex.barbat@upc.edu

method (FEM). Rots and de Borst (1987) and Bazant (1989), among others, have also proposed constitutive models based on CFM.

The possibility to include plasticity, viscoelasticity and damage theories in crack modeling allows developing models based on continuum mechanics. Kachanov (1958) established the basis of the CDM theory that was used later on to represent the mechanical behavior of different materials. The damage model was first applied to represent the dislocation and softening phenomena for metal. Lemaitre (1985) and Simo and Ju (1987; Simo and Ju 1987) proposed the isotropic damaged model; Oliver et al. (1990), Chaboche (1988; Chaboche 1988) and Ju (1989) used CDM for the numerical modeling of quasi-brittle materials. In the early eighties CDM was used for the numerical modeling of concrete. Some of these models were based on CDM and the classical plasticity theory (Jason et al. 2006; Lubliner et al. 1989; Mazars and Pijaudier-Cabot 1989; Oller 1988; Tao and Phillips 2005) among others. The continuum damage constitutive models are defined by using an inner damage variable that represents the deterioration of the strength and the elasticity modulus. This variable can be either scalar or tensorial. In the case of the isotropic damage model (Oliver et al. 1990; Simo and Ju 1987), the inner variable is scalar and, therefore, crack orientation is not considered. If orientation is considered, the local effect of damage becomes anisotropic in nature and the damage variable changes.

When the anisotropy of the damaged and undamaged material is taken into account, the inner variable is defined in the tensorial space by means of a second- or fourth-order tensor (Carol et al. 2002; Cicekli et al. 2007; Ju 1990; Luccioni and Oller 2003; Maire and Chaboche 1997; Martinez et al. 2008). One challenge of the constitutive models based on CDM is modeling the opening and closing of cracks, because the inner damage variable does not decrease. Thereby, constitutive models with two different inner variables, one for tensile damage and another for compressive damage, are necessary when a material is subjected to reversible loads. Mazars and Pujaudier-Cabot (1989) and Faria et al. (1998) proposed constitutive models in which the evolution of each inner variable is activated by using two different threshold functions; these functions, tensile and compressive thresholds, are independent of each other. In the case of axial loads, it is easy to identify if the process is either compressive or tensile, and the results obtained with these models are good; conversely, the results for the shear loads show deficiencies. The tensors of tensile stress and compressive stress are obtained from the polar decomposition of the stress tensor and are compared with the tensile and compressive thresholds, respectively. This fact leads to a discontinuity in the response as well as to an unsuitable representation of shear stresses. However, the independence of the threshold functions in the model of Faria et al. (1998), with two independent threshold functions, has been used in modeling construction joints, in which the tensile strength is near to zero while the compressive strength is high. Paredes et al. (2011) also describe the application of such a model.

In this work, a new constitutive damage model is developed with two scalar inner variables: the tensile damage variable d^+ and the compressive damage variable d^-; the threshold of damage is controlled by only one surface of discontinuity and a new parameter controls the damage variable that should be activated. This new parameter is obtained starting from the model

proposed by Oller (1988) and it is the ratio of tensile stress to compressive stress in the damaged material. This model is based on CDM and complies with the thermodynamics principles of non-reversible, isothermal and adiabatic processes. This new constitutive model with only one damage threshold function is an improvement of the previous conventional $d^+ - d^-$ model of Faria et al. (1998) ensuring the continuity of the response for any type of stress states in each point of analysis. It also introduces a new definition of the internal damage variable and a novel use of the Mohr-Coulomb modified threshold function (Oller et al. 1990).

The model validation is carried out in four sequential steps: 1) the numerical results for increasing monotonic compressive axial loads are compared with the experimental results of Kupfer et al. (1969); 2) the results under the increasing monotonic tensile axial load are compared with the experimental data published by Gopalaratnam and Shah (1985); 3) the numerical results are validated for reversible loads; 4) the results are validated for shear states and compared with the experimental data published by Kupfer et al. (1969). The upgraded model proposed in this article has a unique threshold surface and is oriented towards improving the shear behavior of the original Faria et al. (1998) model. This aspect has been included in page 4 of the new version of the text. The results obtained with the new constitutive model are compared with those of the work of Arrea and Ingraffea (1982), in which a concrete beam was subjected to complex loading. From a fracture mechanics point of view, this test shows the evolution of cracking for the mixed mode fracture.

CONSTITUTIVE TENSION-COMPRESSION DAMAGE MODEL

The aim of the proposed model is to describe the opening, closing and reopening of cracks. Also, this model has been developed to compute stiffness degradation due to the cracking process considering reversible loads. Then, the proposed model allows developing load-displacement curves with high accuracy, even when the load orientation changes. This is the result of proposing a model that is able to recover the stiffness when the load orientation is changed. Nevertheless, the cyclic effect is not taken into account because the model does not incorporate the kinematic hardening effect.

Two concepts have to be defined when formulating the new constitutive damage model for tension (**structural damage**) and compression (**constitutive damage**) behaviors (Paredes 2011). Structural damage is associated with the tensile damage (opening of cracks) suffered by the material at any point; this damage does not imply a decrease of compressive strength during subsequent load states. Thus, the structure is able to support a compressive state after a tensile state. The constitutive damage is associated with the compressive damage (crushing) suffered by the material at any point. The material's compressive failure is a mechanical process that implies its degradation on the constitutive level and, consequently, both the tensile and the compressive strengths decrease.

The Cauchy stress tensor is defined by using the effective stress introduced by Kachanov (1958), also used in the isotropic damage theory (Oliver et al. 1990; Oller 2001). In this work, the Cauchy stress tensor σ is defined by the polar decomposition of the effective stress tensor

σ_o in terms of the tensile damage variable d^+ and the compressive damage variable d^- (Faria et al. 1998) (Wu et al. 2006) (Cicekli et al. 2007)

$$\sigma = (1-d^+)\sigma_o^+ + (1-d^-)\sigma_o^- \tag{1}$$

The tensile stress tensor σ_o^+ and the compressive stress tensor σ_o^-, which are obtained by the polar decomposition of the effective stress tensor σ_o, is expressed as

$$\sigma_o^+ = \sum_{i=1}^{3} \langle \sigma_{oi} \rangle vp_i \otimes vp_i \tag{2}$$

$$\sigma_o^- = \sigma_o - \sigma_o^+ \tag{3}$$

where $\langle \sigma_{oi} \rangle$ is the Macaulay function of the *i*-th principal stress of the effective stress tensor σ_o, and vp_i is the corresponding principal direction. Thus, the effective stress tensor is

$$\sigma_o = C_o : \varepsilon = \sigma_o^+ + \sigma_o^- \tag{4}$$

where ε is the strain tensor and C_o is the fourth-order elastic constitutive tensor of the undamaged material. The tensor σ_o^+ can be also represented by means of the projection tensor

$P = \sum_{i=1}^{3} H(\sigma_{0i}) vp_i \otimes vp_i$

$$\sigma_o^+ = P : \sigma_o$$
$$\sigma_o^- = (I - P) : \sigma_o \tag{5}$$

where $H(\sigma_{0i})$ is the Heaviside function. The initial hypothesis is given by equation (1), which must be tested after ensuring that the constitutive model complies with the thermodynamics principles of non-reversible, isothermal and adiabatic processes.

Thermodynamic framework

Definition of the Helmholtz free energy

By using the mechanical process of tension-compression damage, the Helmholtz free energy is written in the following additive form as it can be seen in references Faria et al. (1998), Wu et al. (2006), Cicekli et al. (2007)

$$\psi = \psi(\varepsilon, d^+, d^-) = (1-d^+)\psi_o^+(\varepsilon) + (1-d^-)\psi_o^-(\varepsilon) \tag{6}$$

The elastic Helmholtz free energy of the undamaged material, in small strain, is defined as

$$\psi_o(\varepsilon) = \frac{1}{2}\varepsilon : C_o : \varepsilon \tag{7}$$

Considering the symmetry of both C_o and ε, and using equations (4) and (5), equation (7) can be expressed as

$$\psi_o(\varepsilon) = \frac{1}{2}\sigma_o : \varepsilon = \frac{1}{2}(\sigma_o^+ + \sigma_o^-) : \varepsilon \tag{8}$$

whereby, for the undamaged material, the elastic Helmholtz free energy is obtained both for tension and compression (see Figure 1)

$$\psi_o(\varepsilon) = \psi_o^+(\varepsilon) + \psi_o^-(\varepsilon) = \frac{1}{2}\sigma_o^+ : \varepsilon + \frac{1}{2}\sigma_o^- : \varepsilon \tag{9}$$

Definitions of stress and constitutive tensors

The mechanical part of the dissipation must comply with the Clausius-Plank inequality (Maugin 1992) which can be written as

$$\dot{\Xi} = \sigma : \dot{\varepsilon} - \dot{\psi} \geq 0 \tag{10}$$

where the temporal variation of free energy is defined by

$$\dot{\psi} = \frac{\partial\psi}{\partial\varepsilon} : \dot{\varepsilon} - \frac{\partial\psi}{\partial d^+}\dot{d}^+ - \frac{\partial\psi}{\partial d^-}\dot{d}^- \tag{11}$$

The mechanical dissipation $\dot{\Xi}$ is obtained by substituting equation (11) for equation (10) and reordering terms

$$\dot{\Xi} = \left(\sigma - \frac{\partial\psi}{\partial\varepsilon}\right)\dot{\varepsilon} + \frac{\partial\psi}{\partial d^+}\dot{d}^+ + \frac{\partial\psi}{\partial d^-}\dot{d}^- \geq 0 \tag{12}$$

According to the Coleman method (Maugin 1992), the inequality (12) holds for all temporal variations of the free variable ε and, therefore, the term $\sigma - \frac{\partial\psi}{\partial\varepsilon}$ must be null. The hyperelastic constitutive law for the model is thus deduced.

$$\sigma = \frac{\partial\psi}{\partial\varepsilon} \tag{13}$$

The mechanical dissipation and, consequently, the expression of hyperelastic constitutive law is obtained, in terms of the inner damage variables d^+ and d^- and of the free variable ε, by substituting equation (6) for equation (13)

$$\sigma = \frac{\partial\psi(\varepsilon, d^+, d^-)}{\partial\varepsilon} = (1-d^+)\frac{\partial\psi_o^+}{\partial\varepsilon} + (1-d^-)\frac{\partial\psi_o^-}{\partial\varepsilon} \tag{14}$$

From equation (9) the free energies for tension and compression are obtained as

$$\psi_o^+(\varepsilon) = \frac{1}{2}\sigma_o^+ : \varepsilon$$

$$\psi_o^-(\varepsilon) = \frac{1}{2}\sigma_o^- : \varepsilon \tag{15}$$

The constitutive equation of the model is obtained by substituting equation (15) for equation (14) and differentiating with respect to the free variable as it can be seen in references Faria et al. (1998), Wu et al. (2006), Cicekli et al. (2007)

$$\sigma = \frac{\partial \psi(\varepsilon, d^+, d^-)}{\partial \varepsilon} = (1-d^+)\sigma_o^+ + (1-d^-)\sigma_o^- \tag{16}$$

The starting hypothesis is confirmed by equation (16) and the mechanical dissipation is expressed as

$$\dot{\Xi} = \psi_o^+ \dot{d}^+ + \psi_o^- \dot{d}^- \geq 0 \tag{17}$$

In equation (17), each term is bigger or equal to zero for all the instants of the process. The general expression of the secant constitutive tensor of the differentiated damaged model is obtained from equation (13)

$$C^s = \frac{\partial \sigma}{\partial \varepsilon} = (1-d^+)\frac{\partial^2 \psi_o^+}{\partial \varepsilon \otimes \partial \varepsilon} + (1-d^-)\frac{\partial^2 \psi_o^-}{\partial \varepsilon \otimes \partial \varepsilon} \tag{18}$$

Damage threshold criterion

For any stress tensor, the damage threshold criterion allows establishing the limit up to which the mechanical behavior is elastic

$$F(\sigma_o, d^+, d^-, r) = f(\sigma_o) - [1 - H(r, R_0)]c^c - [H(r, R_0)]c^t \leq 0 \tag{19}$$

where $f(\sigma_o)$ is a scalar function of the effective stress tensor (equation 4); $c^c = c^c(d^+, d^-, r)$ and $c^t = c^t(d^+, d^-, r)$ are two functions that define either tensile or compressive strength depending on the parameter r; $H(r, R_0)$ is the Heaviside function; $R_0 = \frac{f_o^c}{f_o^t}$ is the ratio of the compressive initial strength of the material to the initial tensile strength; the new parameter $r(d^+, r_o)$ establishes the ratio of the tensile stress to the compression stress for complex stress states; r depends on the inner tensile damage d^+ and on the parameter that establishes if the stresses are tensile or/and compression stresses (Oller 1988). This parameter, named r_o, is an indicator of the tension-compression ratio is written as

$$r_o = \frac{\displaystyle\sum_{i=1}^{3}\langle \sigma_i^o \rangle}{\displaystyle\sum_{i=1}^{3}\left|\sigma_i^o\right|} \tag{20}$$

where $\langle \sigma_i^o \rangle$ is the Macaulay function of the i-th principal stress of the effective stress tensor σ_o. Note that if $r_o = 1$, the stress state represents a pure tension one and, if $r_o = 0$, the stress state represents a pure compression one; if $0 < r_o < 1$ the stress state is complex with tensions and compressions.

In concrete, in which tensile strength is smaller than compressive strength, the degradation of the material under complex stress states starts with the cracking process due to tensile stress. This process changes the configuration of the material from undamaged to damaged and, consequently, the ratio of tensile to compressive stresses also changes. In the case of the

isotropic damage model, this ratio is maintained constant and the parameter r_o is valid (Oller 1988). However, this ratio is variable in the case of the proposed damage model; therefore, a new parameter is introduced, which depends on the tensile damage variable d^+, and represents the changes in the ratio of tensile to compressive responses

$$r = \frac{\sum_{i=1}^{3}\left\langle(1-d^+)\sigma_i^o\right\rangle}{\sum_{i=1}^{3}\left|\sigma_i^o\right|} = (1-d^+)r_o \tag{21}$$

Due to the differentiate behavior in tension and compression strengths of concrete, the failure will be driven by the tension strength when r_o is greater than $1/R_o$. This condition activates, through the r parameter, the internal damage tension variable d^+. In the compression case, the failure will activate the internal damage compression variable d^-. For all the intermediate cases, the following approximation of the r variable is proposed:

$$r = \begin{cases} 1 & \text{if } r_o > 1-1/R_o \\ (1-d^+)r_o & \text{otherwise} \\ 0 & \text{if } r_o < 1/R_o \end{cases} \tag{22}$$

Given that the strain tensor ε is the free variable and that each i-th principal stress of the effective stress tensor σ_i^o represents the response stress of the undamaged material under a complex load state, it can be said that, in an undamaged state, there is proportionality between applied loads and stresses. Consequently, the parameter r_o is an indicator of the tension-compression ratio of both the applied loads and the response stresses.

Once a crack opens, the tension-compression ratio of the stresses must change. This ratio is represented by the new variable r given by equation (22). The use of the ratios r_o and r in the constitutive model allows considering both the complexity of the applied loads and the changes of the mechanical response of the fractured material. As shown in equation (22), in processes with predominant axial loads the ratio r remains constant, whereas in load states with shear actions the ratio r is variable.

The general function that defines the damage threshold given in equation (19) can be particularized for either the tensile damage or the compressive damage function depending on the value of r (see equation 22). The Heaviside function $\mathrm{H}(r, R_0)$ can be defined in terms of r

$$\mathrm{H}(r, R_0) = \begin{cases} 0 & \text{if } r \le \dfrac{1}{R_0} \\ 1 & \text{if } r > \dfrac{1}{R_0} \end{cases} \tag{23}$$

According to equations (22) and (23), the damage threshold criterion for extreme stress states can be written as

$$F(\sigma^o, d^+, d^-, r) = \begin{cases} F^-(\sigma_o, d^+, d^-, r) = f(\sigma_o) - c^c(d^+, d^-, r) \le 0 & \text{if } H(r, R_0) = 0 \\ F^+(\sigma_o, d^+, d^-, r) = f(\sigma_o) - c^t(d^+, d^-, r) \le 0 & \text{if } H(r, R_0) = 1 \end{cases} \tag{24}$$

Compressive damage function: if $H(r, R_0) = 0$, the load process is controlled by the compressive strength of the material; therefore the compressive damage function is given by

$$F^-(\sigma_o, d^+, d^-, r) = G^-\left[f(\sigma_o)\right] - G^-\left[c^c(d^+, d^-, r)\right] \le 0 \tag{25}$$

where $c^c(d^+, d^-, r)$ is the function that defines the compressive damage threshold.

Tensile damage function: if $H(r, R_0) = 1$, the load process is controlled by the tensile strength of the material; in this case the tensile damage function is given by

$$F^+(\sigma_o, d^+, d^-, r) = G^+\left[f(\sigma_o)\right] - G^+\left[c^t(d^+, d^-, r)\right] \le 0 \tag{26}$$

where $c^t(d^+, d^-, r)$ is the function that defines the tensile damage threshold. G^- and G^+ are scalar, invertible, positive, with positive derivatives, and monotonic increasing functions.

The initial values of the threshold functions allow establishing the limit beyond which the behavior will be non-linear. Due to the fact that the ratio of the initial tension strengths to the compression one is R_0, and that this parameter is included in the discontinuity function, the damage model can be formulated in a more objective form using only one initial damage threshold c_o. Normally, this value is defined as the compression strength

$$c_o^c = c_o \tag{27}$$

$$c_o^t = c_o \tag{28}$$

Evolution law of the damage variables of the model

Compressive damage variable

The evolution law of the compressive damage variable can be obtained from the potential

$$\dot{d}^- = \dot{\mu}^- \frac{\partial F^-(f(\sigma_o))}{\partial f(\sigma_o)} \cong \dot{\mu}^- \frac{\partial G^-\left[f(\sigma_o)\right]}{\partial f(\sigma_o)} \tag{29}$$

where $\dot{\mu}^-$ denotes the compressive damage consistency parameter. This parameter allows controlling either the loading or the unloading processes according to the Kuhn-Tucker conditions (Oller 2001)

$$\dot{\mu}^- F^-(\sigma_o, d^+, d^-, r) = 0 \tag{30}$$

From equation (30) it follows that

$$\text{if } F^-(\sigma_o, d^-, r) < 0 \; ; \; \dot{\mu}^- = 0 \Rightarrow d^- = 0 \tag{31}$$

$$\text{if } \dot{\mu}^- > 0 \Rightarrow F^-(\sigma_o, d^-, r) = 0 \; ; \; d^- \ne 0 \tag{32}$$

From the inequality of equation (25) and from the condition established in equation (32), it follows that

$$G^-\left[f(\sigma_o)\right]=G^-\left[c^c(d^+,d^-,r)\right]\Rightarrow f(\sigma_o)=c^c(d^+,d^-,r) \tag{33}$$

Given that function G^- is monotonically increasing, the arguments in equation (33) are equal and, as a consequence, it follows that

$$\frac{\partial G^-\left[f(\sigma_o)\right]}{\partial f(\sigma_o)}=\frac{\partial G^- c^c(d^+,d^-,r)}{\partial c^c(d^+,d^-,r)} \tag{34}$$

From the temporal variation of the compressive damage threshold function, it is obtained that

$$\dot{F}^-(\sigma^o,d^-,r)=\frac{\partial G^-\left[f(\sigma_o)\right]}{\partial f(\sigma_o)}\dot{f}(\sigma_o)=\frac{\partial G^-\left[c^c(d^+,d^-,r)\right]}{\partial c^c(d^+,d^-,r)}\dot{c}^c(d^+,d^-,r) \tag{35}$$

Equation (35) shows that the stress path must remain on the discontinuity surface; therefore, it is possible to conclude that

$$\dot{f}(\sigma_o)=\dot{c}^c(d^+,d^-,r) \tag{36}$$

Additionally, the temporal variation of function G can be expressed as

$$\frac{\partial G^-\left[f(\sigma_o)\right]}{\partial t}=\dot{G}^-\left[f(\sigma_o)\right]=\frac{\partial G^-\left[f(\sigma_o)\right]}{\partial f(\sigma_o)}\dot{f}(\sigma_o) \tag{37}$$

Now, according to equations (29) and (37), $\dot{d}^-=\dot{G}^-$ and, knowing that

$$\dot{\mu}^-=\dot{f}(\sigma_o)=\dot{c}^c(d^-,r) \tag{38}$$

$$\dot{f}(\sigma^o)=\frac{\partial f(\sigma_o)}{\partial\sigma_o}:\dot{\sigma}^o=\frac{\partial f(\sigma_o)}{\partial\sigma_o}:C_o:\dot{\varepsilon} \tag{39}$$

it is possible to obtain the evolution law of the compressive damage variable as

$$\dot{d}^-=\frac{\partial G^-\left[f(\sigma_o)\right]}{\partial f(\sigma_o)}\frac{\partial f(\sigma_o)}{\partial\sigma_o}:C_o:\dot{\varepsilon} \tag{40}$$

The temporal variation of the compressive damage dissipation is obtained from equation (40) and can be written as

$$\dot{\Xi}^-=\psi_o^-\dot{d}^-=\psi_o^-\left\{\frac{\partial G^-\left[f(\sigma_o)\right]}{\partial f(\sigma_o)}\frac{\partial f(\sigma_o)}{\partial\sigma_o}:C_o:\dot{\varepsilon}\right\} \tag{41}$$

Once the non-linearity due to the compressive stress components is reached, the compressive threshold function must be updated in the following form

$$c^c=\max\left\{c_o;f(\sigma_o)\right\}\ \text{if}\ H(r,R_0)=0 \tag{42}$$

Tensile damage variable

The evolution law of the tensile damage variable can be also obtained from the potential function

$$\dot{d}^+=\dot{\mu}^+\frac{\partial G^+\left[f(\sigma_o)\right]}{\partial f(\sigma_o)} \tag{43}$$

Thus, the evolution law of the tensile damage variable can be derived in an analogous way

$$\dot{d}^+ = \left\{ \frac{\partial G^+\left[f(\sigma_o)\right]}{\partial f(\sigma_o)} \frac{\partial f(\sigma_o)}{\partial \sigma_o} : C_o : \dot{\varepsilon} \right\} \tag{44}$$

and the temporal variation of tensile damage dissipation is

$$\dot{\Xi}^+ = \psi_o^+ \dot{d}^+ = \psi_o^+ \left\{ \frac{\partial G^+\left[f(\sigma_o)\right]}{\partial f(\sigma_o)} \frac{\partial f(\sigma_o)}{\partial \sigma_o} : C_o : \dot{\varepsilon} \right\} \tag{45}$$

Once the non-linearity due to the tensile stress components is reached, the tensile threshold function must be updated in the following form

$$c^t = \max\left\{c_o; f(\sigma_o)\right\} \quad \text{if } H(r, R_0) = 1 \tag{46}$$

The tensile damage variable must be updated whenever the compressive damage variable is activated according to the constitutive damage concept

$$d^+ = \max\left\{d^+; d^-\right\} \quad \wedge \quad c^t = \max\left\{c^t; c^c\right\} \tag{47}$$

Finally, the temporal variation of the total mechanical dissipation is obtained as the sum of equations (41) and (45) as shown in equation (12)

$$\dot{\Xi} = \dot{\Xi}^+ + \dot{\Xi}^- \tag{48}$$

PARTICULAR DEFINITIONS OF THE DAMAGE VARIABLES EVOLUTION LAWS

The evolution laws of the tensile and compressive damage variables can be linear, exponential or hyperbolic. Although the discontinuity function $f(\sigma_o)$ is unique, it is possible to consider that each dissipation process (tensile or compressive) may have different evolution laws.

Linear evolution law of the damage variables

The evolution law of the internal damage variables depends on the initial damage threshold c_o for tension and compression and on the values of the tensile and compressive damage thresholds, c^t and c^c, respectively

- *For compression* $d^- \cong G^-\left[c^c(d^+, d^-, r)\right] = 1 - \dfrac{c_o}{c^c(d^+, d^-, r)}$ (49)

- *For tension* $d^+ \cong \max \begin{cases} G^+\left[c^t(d^+, d^-, r)\right] = 1 - \dfrac{c_o}{c^t(d^+, d^-, r)} \\ d^- \end{cases}$ (50)

Exponential evolution law of the damage variables

In the proposed model, the evolution of damage is equal to the evolution of the discontinuity functions and these functions depend on the elastic strain. Therefore, it is possible to use the damage formula of Mazars and Pijaudier-Cabot (Mazars and Pijaudier-Cabot 1989) as given by Faria et al. (1998)

- *For compression*

$$d^- = G^- \left[c^c(d^+, d^-, r) \right] = 1 - \frac{c_o}{c^c}(1 - A^-) - A^- \exp\left(B^-(1 - \frac{c^c}{c_o}) \right); \quad \text{if} \quad c^c \geq c_o \qquad \textbf{(51)}$$

- *For tension*

$$d^+ = \max \begin{cases} G^+ \left[c^t(d^+, d^-, r) \right] = 1 - \frac{c_o}{c^t}(1 - A^+) - A^+ \exp\left(B^+(1 - \frac{c^t}{c_o}) \right); \quad \text{if} \quad c^t \geq c_o \qquad \textbf{(52)} \\ d^- \end{cases}$$

In equations (51) and (52), c_o is the initial damage threshold (for both tension and compression), c^t and c^c are the values of the tensile damage and the compressive damage thresholds, respectively, once non-linearity is reached. A^- and B^- are constants to be obtained from the maximum crashing energy G_c resulting from the uniaxial compressive experimental curve, and A^+ and B^+ are constants to be obtained from the maximum fracture energy G_f resulting from the uniaxial tensile experimental curve. A procedure to obtain these constants can be seen in reference (Paredes et al. 2011). $g_{f/c} = \dfrac{G_{f/c}}{l_{ch}}$ are the regularized crushing g_c/fracture g_c energies of the material and the geometrically regularization parameter l_{ch} called fracture characteristic length related with the size of the finite element makes the non-linear process independent of the used mesh size (Oller 1988; Oliver et al. 1990; Paredes et al. 2011; Oller et al. 1990). The constitutive damage concept introduced above must be complied with, and this is ensured by equations (51) and (52).

Hyperbolic law for damage variables

An objective of the proposed constitutive model is to describe complex stress states, which can be achieved by considering the interaction between tensile and compressive dissipations. By using linear dissipation, the initial ratio of the tension to the compression thresholds is maintained but the hardening effect cannot be represented. Additionally, for compressive dissipation, in the equation proposed by Mazars and Pijaudier-Cabot (1989) the initial compressive strength, σ_o^c, is an input parameter. Thus, by using the constants A^- and B^-, the ultimate compressive strength σ_u^c is internally calculated and the compressive hardening effect is obtained. The tensile dissipation in concrete does not normally show hardening; therefore, the tensile threshold is defined by using the ultimate tensile strength, σ_u^t, instead of the initial tensile strength, σ_o^t. Thus, the operative problem is that two different initial strengths are necessary, σ_o^c for compression and σ_u^t for tension. The goal of this article is to define only one initial strength threshold and to represent the tensile and compressive hardenings by using the following hyperbolic dissipation law

- *For compression*

$$d^- = G^- \left[c^c(d^+, d^-, r) \right] = 1 - (1-q) \frac{e^{k1}}{e^{k1} + e^{-k1}} - q \frac{e^{k2}}{e^{k2} + e^{-k2}}; \quad \text{if} \quad c^c \geq c_o$$

$$k1^- = A1^- \left[\frac{c^c - \left(1 + \frac{5}{A1^-}\right)(c_o)}{c_o} \right]; \quad k2^- = A2^- \left[\frac{(c^c)^2 - \left(1 + \frac{5}{A2^-}\right)(c_o)^2}{(c^c)(c_o)} \right] \quad \textbf{(53)}$$

- *For tension*

$$d^+ = G^+ \left[c^t(d^+, d^-, r) \right] = 1 - (1-q) \frac{e^{k1}}{e^{k1} + e^{-k1}} - q \frac{e^{k2}}{e^{k2} + e^{-k2}}; \quad \text{if} \quad c^t \geq c_o$$

$$k1^+ = A1^+ \left[\frac{c^t - \left(1 + \frac{5}{A1^+}\right)(c_o)}{c_o} \right]; \quad k2^+ = A2^+ \left[\frac{(c^t)^2 - \left(1 + \frac{5}{A2^+}\right)(c_o)^2}{(c^t)(c_o)} \right] \quad \textbf{(54)}$$

where c_o is the initial damage threshold (for both tension and compression) that is normally given by the compressive strength of the material; $Ai^\pm$ and q are constants that must be obtained from experimental studies. Similarly as explained in section treating the "Exponential evolution law of the damage variables", the objectivity of the mesh has been reached including the regularized fracture and crashing energy in the parameters $Ai^\pm$.

DISCONTINUITY STRESS FUNCTION

Several discontinuity functions can be used within the proposed differentiated damage model. The discontinuity function must be chosen assuring the best representation of the behavior of each material. The modified Mohr-Coulomb discontinuity function (Oller 1991) will be used in the implementation and validation of the proposed constitutive model. The modified Mohr-Coulomb function is suitable to represent the mechanical behavior of concrete because it allows considering the ratio R_o. It depends on the effective stress tensor and is given by

$$f(\sigma_o) = f(I, J_2, \theta, \phi) = \left\{ \frac{I}{3} K_3 + \sqrt{J_2} \left[K_1 \cos(\theta) - K_2 \frac{\sin(\theta)\sin(\phi)}{\sqrt{J_3}} \right] \right\} \frac{2\sqrt{N_\phi}}{\cos(\theta)} \quad \textbf{(55)}$$

Thus, the threshold function defined in equation (19) can be written as

$$F(\sigma_o, d^+, d^-, r) = f(I, J_2, \theta, \phi) - c_o = 0 \quad \textbf{(56)}$$

where $c_o = \sigma_o^c$ is the compressive strength of concrete. The constants defined in equation (55) can be expressed as

12

$$K_1 = \left[\frac{1+\alpha}{2} - \frac{1-\alpha}{2} \sin\phi \right] \; ; K_2 = \left[\frac{1+\alpha}{2} - \frac{1-\alpha}{2} \frac{1}{\sin\phi} \right]$$

$$K_3 = \left[\frac{1+\alpha}{2} \sin\phi - \frac{1-\alpha}{2} \right] \tag{57}$$

$$R_o = \left| \frac{f_o^c}{f_o^t} \right| \quad ; \quad \alpha = \frac{R_o}{N_\phi} \quad ; \quad N_\phi = \tan^2\left[\frac{\pi}{4} + \frac{\phi}{2} \right]$$

INTEGRATION ALGORITHM OF THE PROPOSED CONSTITUTIVE MODEL

The procedure that allows integrating the proposed constitutive law is explained in Figure 2. From the mechanical properties of the material, the initial threshold c_o is established, which is common to both compression and tension processes. The non-linear process should be carried out step by step with increasing load increments. Thus, for the i-th load increment and for an analysis point, the input values for both the inner damage variables $^{i-1}d^+$ and $^{i-1}d^-$, and the thresholds $^{i-1}c^+$ and $^{i-1}c^-$, must be given in the previous step; the strain tensor ε is the free variable that allows calculating the effective stress tensor σ_o, with which the tensile and the compressive stress tensors can be calculated through polar decomposition (see equations 2 and 3). Thus, the stress ratio r and the Heaviside function $\mathrm{H}(r, R_0)$ are obtained (see equations 22 and 23, respectively). The value of the discontinuity function $f(\sigma_o)$ is obtained from the effective stress tensor σ_o. The type of damage (tensile or compressive) must be established depending on the value of the Heaviside function $\mathrm{H}(r, R_0)$, and the discontinuity function is compared with either the $^{i-1}c^t$ or $^{i-1}c^c$ threshold values. The above procedure must be carried out for all the material analysis points and, subsequently, the global convergence must be verified through integration in the space domain. Once convergence is achieved, the next load step will be applied; otherwise, the iterative process must be carried out and the above procedure will restart.

VALIDATION OF THE PROPOSED MODEL

The proposed model was implemented in the finite element software PLCD (PLCD-Manual 2008) and validated by comparing the numerical result with experimental data obtained from the literature. Several tests were performed, including the compressive axial test, the tensile axial test, the reversible axial test and the biaxial test.

Monotonic compressive axial load

The response of the model was validated by comparing the numerical results with one of the most invoked experimental results, published by Kupfer et al. (1969). The friction boundary condition of the experimental test at the ends of the sample was not considered in the numerical analysis. The experimental results are shown in Figure 3 and correspond to an elastic modulus

$E = 28657000 \text{ kPa}$, an initial compressive strength $f_o^c = 13120 \text{ kPa}$, and an ultimate compressive strength $f_u^c = 32800 \text{ kPa}$ and also $A^- = 1.38$ and $B^- = 0.22$ (see equation 51). Using this data, monotonic compressive axial loads were applied numerically on a 0.20 x 0.20 x 0.05 m concrete sample discretized in hexahedral-shaped finite elements; similar result to that obtained by Kupfer have been obtained. The linear dissipation curve is fitted in such a way that the energy dissipated per unit volume was equal to that obtained by using the exponential dissipation curve, when both curves have the same compression threshold. For each area under the curve (see Figure 4), dimensions of the element, and the compression/ tension ratio of the material ($R_o = 10$), the value of the fracture energy per surface unit was calculated as $G_f = 0.3$ kNm/m2.

Monotonic tensile axial load

The experimental results obtained by Gopalaratnam and Shah (1985) for a specimen measuring 76 x 19 x 305 mm with notches of 13 x 3 mm on each side were used to validate the model under monotonic tensile axial loads. Thus, the effective area perpendicular to the direction of the tensile load is 50 x 19 mm. Measurements of the longitudinal displacements were made using two sets of strain gages that were 13 and 83 mm long. In order to take full advantage of the experiment, a numerical model of 50 x 19 x 83 mm was selected. The mechanical properties of the material to be used in numerical analysis were directly obtained from reference (Gopalaratnam and Shah 1985), excepting the fracture energy per unit area, G_f, which was calculated as the area below the experimental stress-displacement curve. These properties are shown in Table 1. Numerical analysis considering the dissipation laws described above was carried out. Incremental displacements in the longitudinal direction, δ_z, were applied at the top face while the displacements at the bottom were restricted to ensure axiality. The numerical force-displacement curves fitted the experimental ones quite accurately, as seen in Figure 5. Similar results are shown for the stress-displacement curves (Figure 6) and the stress-strain curves (Figure 7). The fracture energy per unit area was calculated for each dissipation law and these results are shown in Table 2.

Mesh objectivity

Objectivity was studied using three different meshes for the same specimen: mesh 1 with 312 elements and 504 nodes, mesh 2 with 680 elements and 990 nodes, and mesh 3 with a single-element and 4 nodes. Incremental displacements in the longitudinal direction, δ_z, were applied on the top nodes, whereas displacements on the bottom nodes have been restricted in order to ensure axiality. Geometry, meshes and boundary conditions are shown in Figure 8. Each force-displacement curve fits each other accurately for the three analyzed meshes (see Figure 9). Thus, it can be concluded that the proposed model meets the requirements of mesh objectivity and the dissipated energy is independent of the size of the mesh.

14

Reversible loads test

This test shows that, under a reversible load, the model maintains the stiffness to compression after being damaged to tension. Many models can simulate this effect but the one proposed has a distinctive feature: it defines the damage space with a single discontinuity threshold function. This fact allows using the classic functions of Mohr-Coulomb, Modified Mohr Coulomb, Drucker-Prager etc. Nevertheless, it is important to note that the damage to compression can be visualized by following the loading-unloading path shown in Figures 10-12.

The model's response under uniaxial reversible loads was tested. The loads were applied on a single element of concrete and started with tension, followed by compression. The tensile load was increased up to the tensile damage threshold (o-a) and the softening effect was numerically observed as the tensile damage variable grew (a-b). The tensile unloading process was then carried out (b-o), followed by a compressive load increase beyond the compressive damage threshold (o-c-d). Then, the compressive unloading process was carried out (d-o). The tensile reload was increased beyond the last tensile damage threshold (o-b-e). Then the tensile unloading process was repeated (e-o), followed by a compressive reload beyond the last compressive damage threshold (o-f-g). After that, compressive unload (g-o) and tensile reload (o-h-i) followed.

The tensile damage was activated in a-b; however, the compressive load (o-c) occurred with the undamaged stiffness of the material. The tensile crack opened in a-b, and, subsequently, this crack closed in b-o. The initial compressive strength and the initial compressive stiffness of the material were maintained in o-c, whereas the compressive damage variable remained null. The compressive damage variable grew on c-d; however, the tensile damage variable at point b was greater than the compressive damage variable at point d. Therefore, the slope of compressive unload (d-o) was greater than the slope of tensile reload (o-b). It can be said that the structural damage occurred up to point d, which explains the structural damage concept that was introduced earlier. The evolution of the tensile damage variable depends on the load path and can be seen in Figure 11.

The compressive damage variable at point f was smaller than the tensile damage variable at point e. The compressive load was applied on f-g; then, the compressive damage value reached the last tensile damage value (point e) during path f-g. Thereafter, the evolution of the tensile damage variable must be equal to the evolution of the compressive damage. This implies that the slope of the tensile reload path o-h must be equal to the slope of the compressive unload path g-o. Note that the tensile damage variable at point h is greater than at point e without applying tensile load. Therefore, there is a discontinuity between points e and h. All this explains the constitutive damage concept that was introduced before. The evolution of the compressive damage variable depends on the load path and can be seen in Figure 12.

According to Figures 10-12, it is possible to remark that compressive damage introduces tensile damage, whereas tensile damage does not introduce compressive damage.

Analysis under biaxial loads

The ability of the model to analyze biaxial problems was validated following the experimental results of Kupfer et al. (1969). The biaxial test was performed on the same specimen described before. The specimen was simultaneously subjected to tensile σ_1 and compressive σ_2 stresses. Numerical analysis was carried out for several σ_2/σ_1 ratios whose results are shown in Figure 13, where stress strain curves for both tensions and compressions can be seen.

Strength curves for concrete under combined tension and compression were published by Kupfer et al. (1969) for three values of the ultimate compressive strength of concrete $\sigma_u = 190$ kg/cm^2, $\sigma_u = 315$ kg/cm^2 and $\sigma_u = 590$ kg/cm^2. Numerical results were obtained for $\sigma_u = 328$ kg/cm^2, in agreement with the shear experimental results shown in Figure 14. The proposed constitutive model yields better results under complex loads, which is one advantage for concrete modeling. Additionally, this allows representing the sequence of both cracking and crushing processes in coupled form.

The failure sequence has been analyzed in the case of pure shear ($\sigma_2/\sigma_1 = -1/1$). Tension and compression dissipation are shown in Figure 15. It can be observed that, if the threshold function of the material is exceeded (a_t or a_c), the tensile strength decreases (segment a_t - b_t) as tensile damage variable starts to increase, whereas compressive strength continues to increase (segment a_c - b_c) up to point b_c. At this point, the compressive damage variable is activated because the tension-compression ratio r has changed. Variable r becomes smaller than parameter $1/R_0$ along b_t-c_t, (see equation 22). Therefore, the value of the Heaviside function must be changed (see equation 23) and the compressive threshold is activated (see equation 24). From this point (c_t or c_c), the tensile and compressive damage variables will grow at the same rate, as it is a constitutive damage. This behavior was compared with both the isotropic damage model (Oller 1991) and the constitutive damage model proposed by Faria et al. (1998). Thereafter, the threshold function of the material is exceeded (points a_t and a_c) and softening for both tension and (a_t-c_t) compression (a_c-c_c) occurs, as seen in Figure 15. The constitutive damage model proposed by Faria et al. (1998) indicates that there are two failure points: when the principal tensile stress reaches the tensile strength of the material; and, subsequently, when the principal compressive stress reaches the compressive strength of the material. This fact can be explained because two independent threshold functions are used in this model. Thus, tensile and compressive responses will be independent of the σ_2/σ_1 ratio. This new constitutive model allows correcting the disadvantages of the numerical modeling of concrete under shear load.

APPLICATION EXAMPLE

Description of the experimental test

The results of the experimental test carried out by Arrea and Ingraffea (1982) will be used herein for the validation of the proposed model. This test has been traditionally used for the validation of constitutive models of concrete (Blanco Ibáñez 2007; Gálvez and Cendón 2002; Oller 1988; Rots and de-Borst 1987). Two concentrated loads are applied on the beam, which are asymmetric with respect to the notch and the supports. The ratio between these loads is 0.13/1 and was maintained by using a high-stiffness beam. The punching effect on the loading and support points was avoided in the test by using steel plates to distribute the forces. Each loading step has three different stages. First, the load is increased, then the load is maintained constant, and, finally, it is removed. The experimental test made by Arrea and Ingraffea (1982) was carried out using two types of concrete with compressive strengths of $f_o^c = 45.5 \, \text{MPa}$ and $f_o^c = 43.4 \, \text{MPa}$ (series B and series C, respectively). Each series has a different kind of notch but the notch depth is 82 mm in both series. The geometry of the test beam is shown in Figure 16.

Numerical analysis

The concrete beam in Figure 16 is discretized using 13014 linear tetrahedral elements with only one integration point. The mesh with 2.842 nodes is shown in Figure 17a. The forces in points A and B were applied in 63 incremental steps. The arc-length method is employed when the softening response is reached, and the crack mouth sliding displacement, CMSD, is the control parameter. Ten pairs of nodes were controlled, located on the lips of the notch. Longitudinal (x direction) and vertical (z direction) displacements of the nodes in line D were restricted, whereas the displacements of the nodes in line E were only restricted in the vertical direction z. The applied loads and support conditions are shown in Figure 17b.

Input parameters

A numerical analysis was carried out using the input parameters of the Arrea and Ingraffea test (Arrea and Ingraffea 1982): the compressive strength of concrete $f_o^c = 43.4 \, \text{MPa}$, the elasticity modulus $E = 43.4 \, \text{GPa}$ and the Poisson coefficient $\upsilon = 0.18$. Additionally, the tensile strengths of concrete, f_o^t, with values between 2715.5 and 2630.3 kPa, were calculated depending on the parameter $R_0 = f_o^c / f_o^t$, and for the energy of fracture per unit area, G_f, values between 0.045 and 0.065 kNm/m^2 were used. For the numerical validation of the model it was necessary to carry out the sensitivity analysis for different concrete properties (see Table 3) because neither tensile strength nor energy of fracture is known for the experimental data.

Results

Numerical results obtained with the new constitutive tension-compression damage model agree with the experimental results published by Arrea and Ingraffea (1982) quite accurately. The results obtained by using the proposed model were compared with both the numerical results reported by Oller (1988) (see Figure 18) and the numerical results published by Gálves and Cendón (2002) (see Figure 19), which agree quite well. The objective of Figures 18 and 19 is to illustrate the sensitivity of the results to several combination of fracture energy G_f with tensile strength f_o^t. The curves P'- CMSD are plotted for the total vertical reaction force, P'.

In the DCM theory, the evolution from microcracks to cracks is represented by the evolution of the inner damage variables. The damage value for which microcracks become cracks is not defined and it is still a topic of discussion. However, it is possible to consider that the evolution of the inner damage variable corresponds to the area in a structural element where microcracks and cracks are located.

The numerical results for the damage variables show that the cracking pattern in the experimental beam fits the envelope of cracks drawn by Arrea and Ingraffea (1982). The numerical and experimental cracking patterns are overlapped in Figure 20. The evolution of the tensile damage variable started in load step 5; the major value of tensile damage variable was 0.1731 for this load step. In load step 13, a peak vertical reaction of 166.78 kN was reached, which corresponded to a value of the tensile damage variable of 0.9247 (see Figures 18, 19 and 21). Subsequently, the descending branch of the P'-CMSD curve starts in load step 23 and becomes gradually asymptotic in load step 45 (see Figures 18 and 19). The last load step was 63, for which the highest value of the tensile damage variable was 0.9959. The evolution of the tensile damage variable is shown in Figure 21 and the cracking process corresponds to mode II of fracture in shear up to load step 13. However, there is compressive stress on the faces of the notch, which implies that there could be compressive damage in this zone. In step 23 (see Figure 21), it can be seen that the notch is open. Notice that between steps 13 and 23 there was a change in the fracture mode, from mode I to the mixed mode, due to the fact that the fracture zone is subjected to shear and tensile stresses. Thereafter, in steps 45 and 63, the fracture zone grows following the described mechanism, although tensile stress is predominant for these steps.

In step 13 the compressive damage variable had a value of 0.1325, which grew up to 0.6884 in step 63. As shown in Figure 22, compressive damage is present at the top of the notch due to the fact that shear and compressive stresses are concentrated there during the first steps. That is, this zone is subjected to complex load states. In the final steps, compressive damage is observed at the top of the fractured zone due to the fact that the compressive stress necessary for the beam equilibrium is high. The evolution of the compressive damage variable is shown in Figure 22.

The proposed constitutive tension-compression damage model is based on the CDM theory, where fracture is not considered as a discontinuity of the continuum medium, but rather as a discontinuity in the displacement field. It is known that discontinuity in a displacement field

implies a strong discontinuity in the strain field. The numerical results are in agreement with this premise, which can also be seen in the experimental fracture zone (see Figure 23)

The load state and the support conditions imposed on the beam produce a complex stress state in the failure zone. The shear actions are predominating, and there is stress concentration particularly at the top of the notch, where stress states become complex in nature. Therefore, the principal stress fields must be examined in order to understand the response of each analyzed element. The maximum principal stress field (tensions) and the minimum principal stress field (compressions) observed in load step 13 are shown in Figure 24, where it is also possible to observe that the highest maximum principal stress has a value of 3.3 MPa, whereas the highest minimum principal stress has a value of -19.244 MPa. The values of both principal stresses are relatively high around the top notch; this fact confirms that, in this zone, the stress state is complex in nature. The compressive damage variable begins its evolution in step 13 (see Figure 22) after the tensile damage variable had started its evolution in step 5 (see Figure 21).

CONCLUSIONS

A new constitutive damage model with compressive and tensile damage variables using only one discontinuity surface has been proposed. An adequate response of the model under shear, tensile, compressive, biaxial and complex loads allows coming to the conclusion that the proposed model is a powerful tool for the numerical modeling of reinforced concrete structures.

The discontinuity function depends only on the effective stress tensor. Therefore, the continuity of the response is ensured even if polar decomposition of the effective stress tensor is mandatory in order to calculate both the tensile and the compressive damage variables. This means, however, that tensile and compressive problems were analyzed as a single mechanical problem.

Because tensile and compressive damage variables were defined, it is possible to represent the mixed mode of fracture (typical of CFM) through a CDM perspective. This was achieved by using an adequate evolution law for the damage variables.

The proposed model is based on the CDM theory, where fracture is not considered as a discontinuity of the continuum medium, but rather as a discontinuity in the displacements field. The numerical results are in agreement with this premise, which can be seen in the application examples where the discontinuity in the displacement field in the experimental beam fits the enveloping of the experimental cracks.

The inner damage variables have been considered as scalar, which do not allow determining the cracking pattern associated with an orientation. Therefore, the development of a damage model with the damage variables defined at a vectorial or tensorial order, and with only one discontinuity function, would be an important research topic in the future.

REFERENCES

Arrea, M., and Ingraffea, A. (1982). "Mixed Mode Crack Propagation in Morar and Concrete." *Tecnical report 81-13*, Dpt. of Structural Engineering, Cornell University.

Bazant, Z. P., and Pijaudier-Cabot, G. (1989). "Measurement of Characteristic Length of Nonlocal Continuum." *Journal of Engineering Mechanics*, 115(4), 755-767.

Blanco Ibáñez, S. (2007). "Contribuciones a la simulación numérica del fallo material en medios tridimensionales mediante la metodología de discontinuidades fuertes de continuo." Ph.D. Thesis (in Spanish), Universitat Politècnica de Catalunya, Barcelona.

Carol, I., Rizzi, E., and Willam, K. (2002). "An 'extended' volumetric/deviatoric formulation of anisotropic damage based on a pseudo-log rate." *European Journal of Mechanics - A/Solids*, 21(5), 747-772.

Cicekli, U., Voyiadjis, G. Z., and Abu Al-Rub, R. K. (2007). "A plasticity and anisotropic damage model for plain concrete." *International Journal of Plasticity*, 23(10-11), 1874-1900.

Chaboche, J. L. (1988). "Continuum Damage Mechanics: Part I-General Concepts." *Journal of Applied Mechanics*, 55(1), 59-64.

Chaboche, J. L. (1988). "Continuum Damage Mechanics: Part II-Damage Growth, Crack Initiation, and Crack Growth." *Journal of Applied Mechanics*, 55(1), 65-72.

Faria, R., Oliver, J., and Cervera, M. (1998). "A strain-based plastic viscous-damage model for massive concrete structures." *International Journal of Solids and Structures*, 35(14), 1533-1558.

Gálvez, J. C., and Cendón, D. A. (2002). "Simulación de la fractura del hormigón en modo mixto." *Revista Internacional Métodos numéricos para cálculo y diseño en ingeniería*, 118(1), (in Spanish).

Gopalaratnam, V. S., and Shah, S. P. (1985). "Softening response of plain concrete in direct tension." *Journal of the American Concrete Institute.*, 82(27), 310-321.

Hillerborg, A., Modéer, M., and Petersson, P. E. (1976). "Analysis of crack formation and crack growth in concrete by means of fracture mechanics and finite elements." *Cement and Concrete Research*, 6(6), 773-781.

Jason, L., Huerta, A., Pijaudier-Cabot, G., and Ghavamian, S. (2006). "An elastic plastic damage formulation for concrete: Application to elementary tests and comparison with an

isotropic damage model." *Computer Methods in Applied Mechanics and Engineering*, 195(52), 7077-7092.

Ju, J. W. (1989). "On energy-based coupled elastoplastic damage theories: Constitutive modeling and computational aspects." *International Journal of Solids and Structures*, 25(7), 803-833.

Ju, J. W. (1990). "Isotropic and Anisotropic Damage Variables in Continuum Damage Mechanics." *Journal of Engineering Mechanics*, 116(12).

Kachanov, L. M. (1958). "Time of rupture process under creep conditions." *Izvestia Akaademii Nank*, 8, 26-31.

Kupfer, H., Hilsdorf, H., and Rusch, H. (1969). "Behaviour of concrete under biaxial stresses." *Journal of the American Concrete Institute*, 66(8), 656-666.

Lemaitre, J. (1985). "Coupled elasto-plasticity and damage constitutive equations." *Computer Methods in Applied Mechanics and Engineering*, 51(1-3), 31-49.

Lubliner, J., Oliver, J., Oller, S., and Oñate, E. (1989). "A plastic-damage model for concrete." *International Journal of Solids and Structures*, 25(3), 299-326.

Luccioni, B., and Oller, S. (2003). "A directional damage model." *Computer Methods in Applied Mechanics and Engineering*, 192(9-10), 1119-1145.

Maire, J. F., and Chaboche, J. L. (1997). "A new formulation of continuum damage mechanics (CDM) for composite materials." *Aerospace Science and Technology*, 1(4), 247-257.

Martinez, X., Oller, S., Rastellini, F., and Barbat, A. H. (2008). "A numerical procedure simulating RC structures reinforced with FRP using the serial/parallel mixing theory." *Computers & Structures*, 86(15-16), 1604-1618.

Maugin, G. A. (1992). *The thermodynamics of plasticity and fracture*, Cambridge University press.

Mazars, J., and Pijaudier-Cabot, G. (1989). "Continuum Damage Theory -Application to Concrete." *Journal of Engineering Mechanics*, 115(2), 345-365.

Oliver, J., Cervera, M., Oller, S., and Lubliner, J. "Isotropic damage models and smeared crack analysis of concrete." *Proc., Proc. 2nd. Int. Conf. on Computer Aided Analysis and Design of Concrete Structures*, Zell am See, 945-958.

Oller, S. (1988). "Un modelo de daño continuo para materiales-friccionales." Ph.D. Thesis (in Spanish), Universitat Politécnica de Cataluña, Barcelona.

Oller, S. (1991). *Modelización numérica de Materiales Friccionales*, CIMNE, Barcelona.

Oller, S. (2001). "Fractura Mecánica. Un enfoque global.", CIMNE, Barcelona, 200-217.

Paredes, J. A. (2011). "Modelización numérica del comportamiento constitutivo del daño local y global y su correlación con la evolución de las frecuencias naturales en estructuras de hormigón reforzado." Ph.D. Thesis (in Spanish), Universidad Politécnica de Cataluña, Barcelona.

Paredes, J. A., Barbat, A. H., and Oller, S. (2011). "A compression–tension concrete damage model, applied to a wind turbine reinforced concrete tower." *Engineering Structures*, 33(12), 3559-3569.

PLCD-Manual (2008). "Non-linear thermo mechanic finite code element oriented to PhD student education. Code developed at CIMNE."Barcelona.

Rots, J. G., and de-Borst, R. (1987). "Analysis of Mixed-Mode Fracture in Concrete." *Journal of Engineering Mechanics*, 113(11), 1739-1758.

Simo, J. C., and Ju, J. W. (1987). "Strain- and stress-based continuum damage models-I. Formulation." *International Journal of Solids and Structures*, 23(7), 821-840.

Simo, J. C., and Ju, J. W. (1987). "Strain- and stress-based continuum damage models-II. Computational aspects." *International Journal of Solids and Structures*, 23(7), 841-869.

Tao, X., and Phillips, D. V. (2005). "A simplified isotropic damage model for concrete under bi-axial stress states." *Cement and Concrete Composites*, 27(6), 716-726.

Wu, J.Y, Li, J. and Faria R. (2006). "An energy release-based plastic-damage model for concrete". *International Journal of Solids and Structures*, 43, 583-612.

Figures
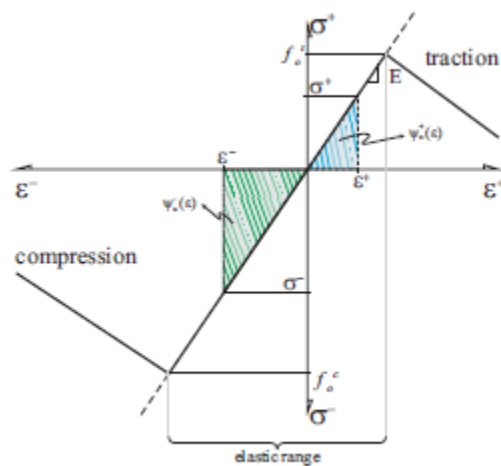
Figure 1. Tension and compression elastic energy.

initial strength threshold of material: c_o

damage variables to step $i\text{-}1$: $^{i\text{-}1}d^+$; $^{i\text{-}1}d^-$;   strength thresholds to step $i\text{-}1$: $^{i\text{-}1}c^+$; $^{i\text{-}1}c^-$

total stain tensor : ε

calculate of effective stress tensor : $\sigma_o = C_o : \varepsilon$

polar decomposition of effective stress tensor
$$\sigma_o^+ = \left\langle \underline{s}_{oi} \right\rangle vp_i \otimes vp_i \qquad \sigma_o^- = \sigma_o - \sigma_o^+$$

calculate of tensile/compressive ratio

$$r_o = \frac{\sum_{i=1}^{3}\langle \underline{s}^o \rangle}{\sum_{i=1}^{3}|\underline{s}^o|}$$

$$r = \begin{cases} 1 & \text{if } r_o > 1 \ 1/R_o \\ (1 - {}^{i\text{-}1}d^+)r_o & \text{Otherwise} \\ 0 & \text{if } r_o < 1/R_o \end{cases}$$

Heaveside function
$$H(r, R_o) = \begin{cases} 0 & \text{if } r \le \dfrac{1}{R_0} \\ 1 & \text{if } r > \dfrac{1}{R_0} \end{cases}$$

Discontinuity function
$$f(\sigma_o) = f(I, J_2, q, f)$$

$f(\sigma_o)$
$H(r, R_o)$

next iteration

new load step i

traction | traccion | compression | compression

pure traction:
$r = 1$; $H(r, R_0) = 1$

traction-compression
$$r = (1 - {}^{i\text{-}1}d^+)r_o \; ; \; H(r, R_0) = \begin{cases} 0 \\ 1 \end{cases}$$

pure compression:
$r = 0$; $H(r, R_0) = 0$

$$F^+(\sigma_o, d^+, d^-, r) = f(\sigma_o) - {}^{i\text{-}1}c^+ \le 0$$
$$d^+ = 1 - \frac{c_o}{{}^{i}c^+}$$
$$^{i}c^+ = \max\left\{ {}^{i\text{-}1}c^+ ; f(\sigma_o) \right\}$$

$$F^-(\sigma_o, d^+, d^-, r) = f(\sigma_o) - {}^{i\text{-}1}c^- \le 0$$
$$d^- = 1 - \frac{c_o}{{}^{i\text{-}1}c^-}$$
$$^{i}c^- = \max\left\{ {}^{i\text{-}1}c^- ; f(\sigma_o) \right\}$$

$$d^+ = \max\left\{ d^+ ; d^- \right\}$$
$$^{i}c^+ = \max\left\{ {}^{i}c^+ ; {}^{i}c^- \right\}$$

$$\sigma = (1 - d^+)\sigma_o^+ + (1 - d^-)\sigma_o^-$$

$$d^+ = d^-$$
$$^{i}c^+ = {}^{i}c^-$$
condition of constitutive damage

integration into espace

NO convergence

convergence verification

Convergence is reached

Figure 2. Constitutive model integration flowchart.
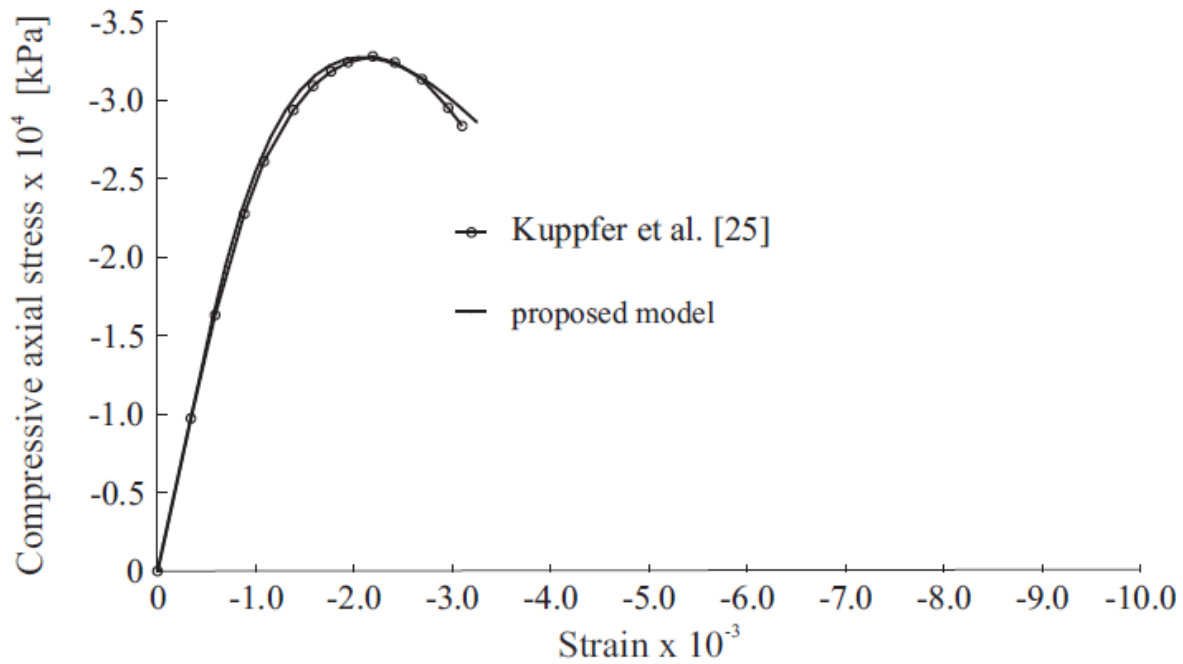
Figure 3. Stress-strain relationship under axial compression compared with the Kupfer experimental curve (Kupfer et al. 1969). $\sigma_1/\sigma_2 = -1/0$.
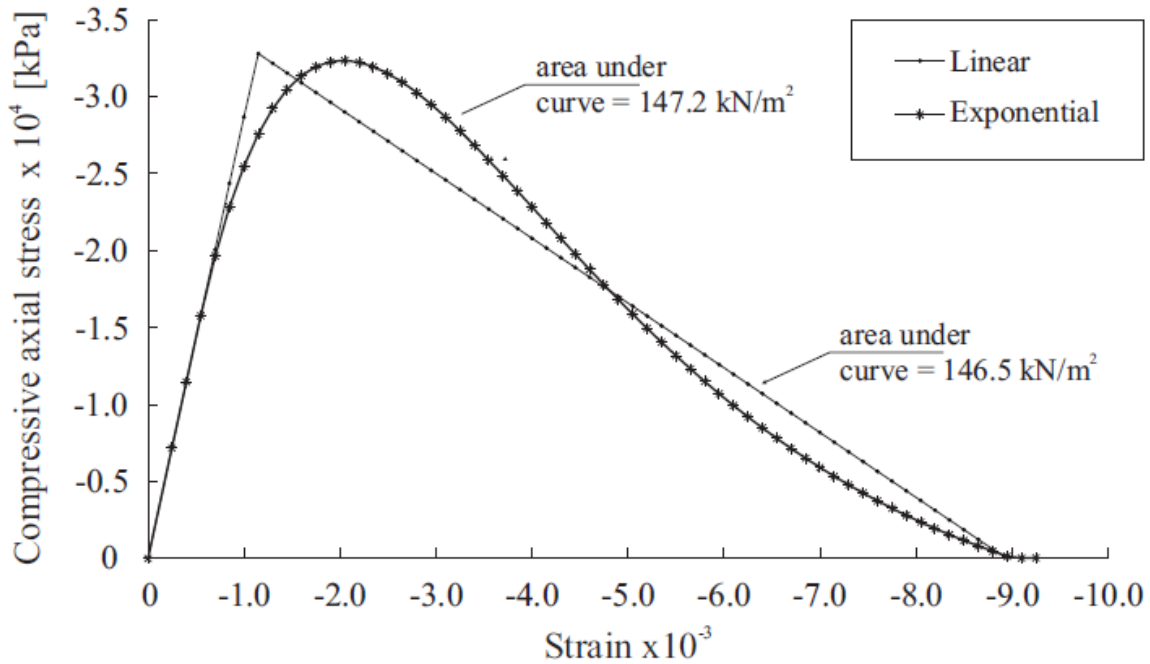
Figure 4. Linear and exponential dissipation under axial compression.
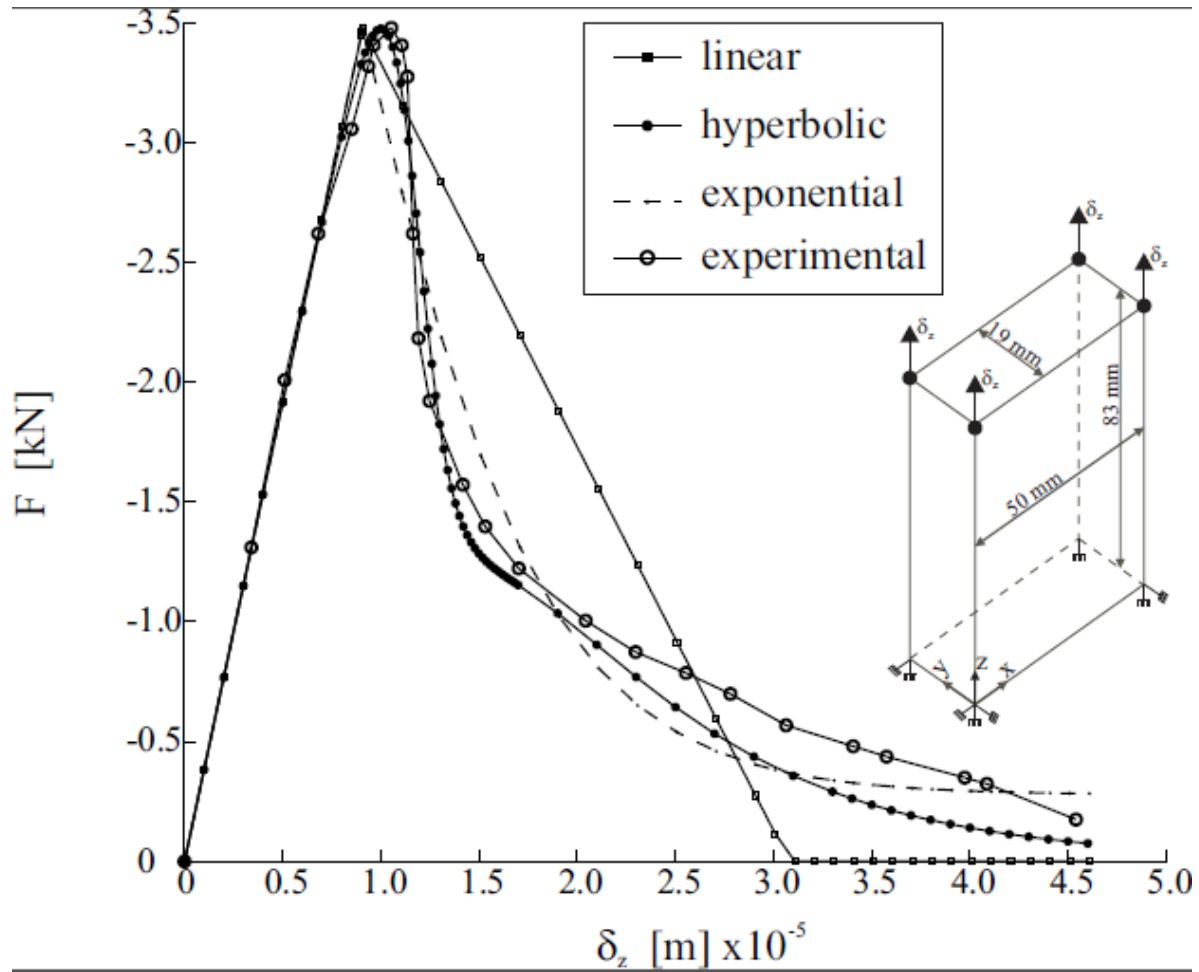
Figure 5. Force-displacement curves. Linear, hyperbolic and exponential dissipation compared with the experimental curve of Gopalaratnam and Shan (1985).
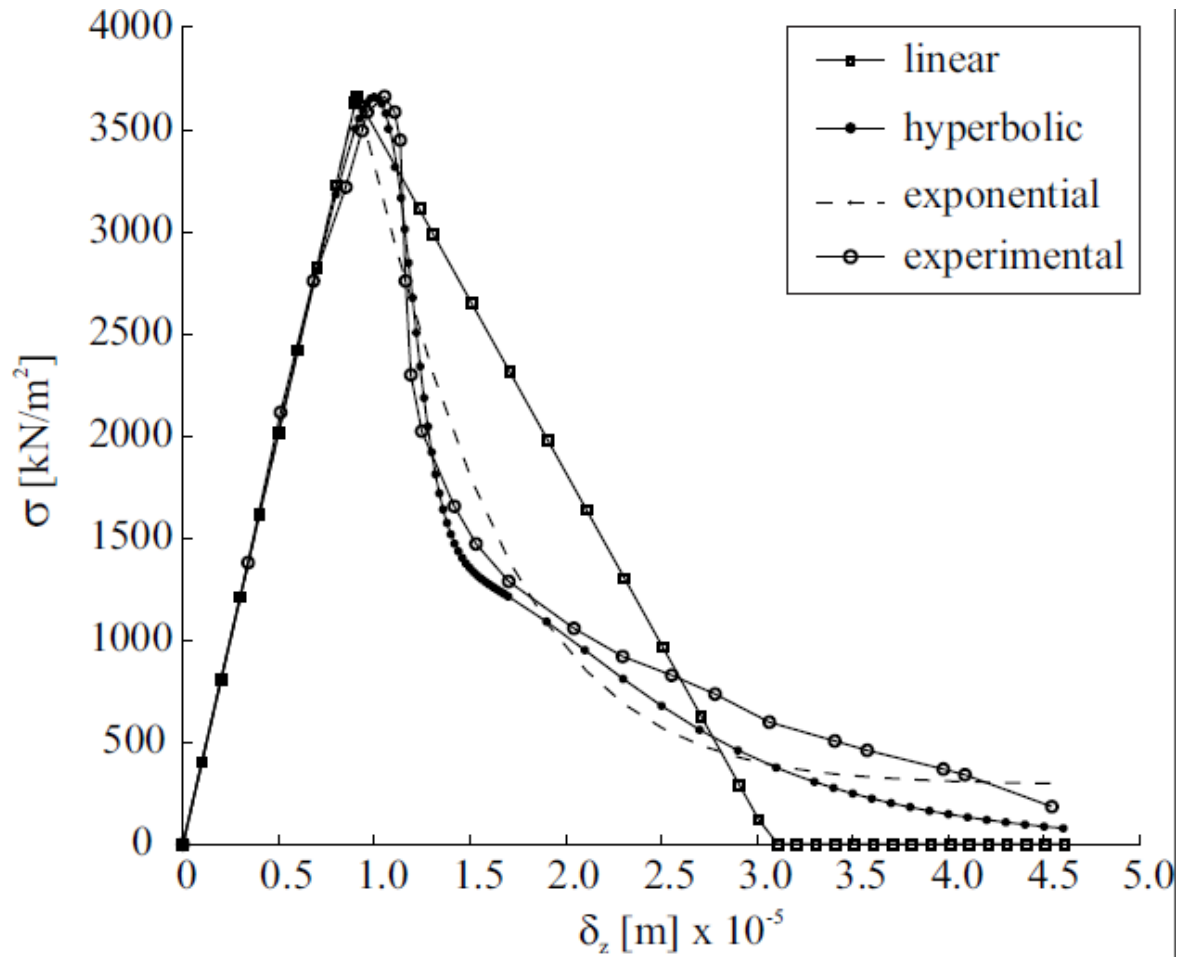
Figure 6. Stress-displacement curves. Linear, hyperbolic and exponential dissipation compared with the experimental curve of Gopalaratnam and Shan (1985).
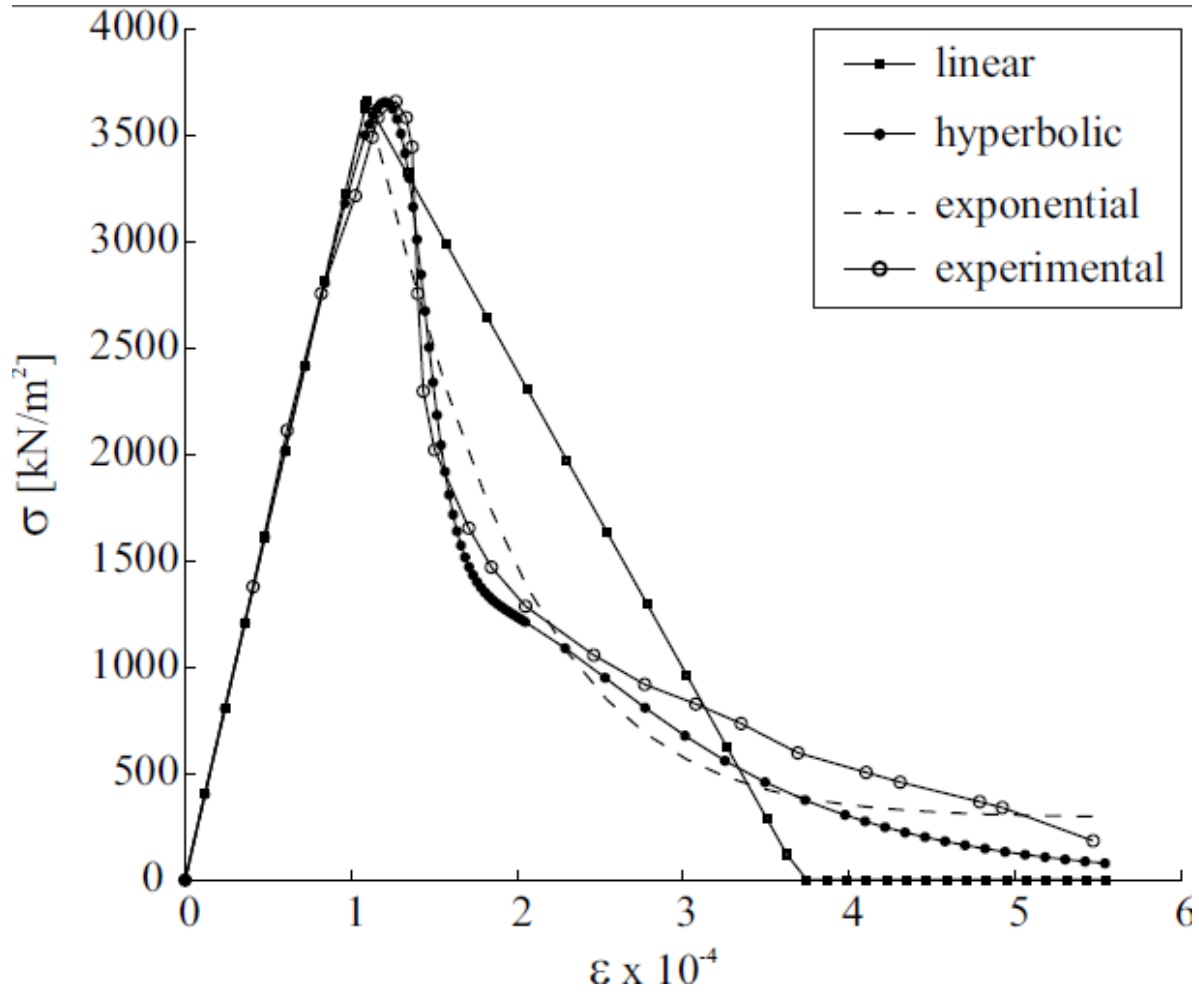
Figure 7. Stress-strain curves. Linear, hyperbolic and exponential dissipation compared with the experimental curve of Gopalaratnam and Shan (1985).
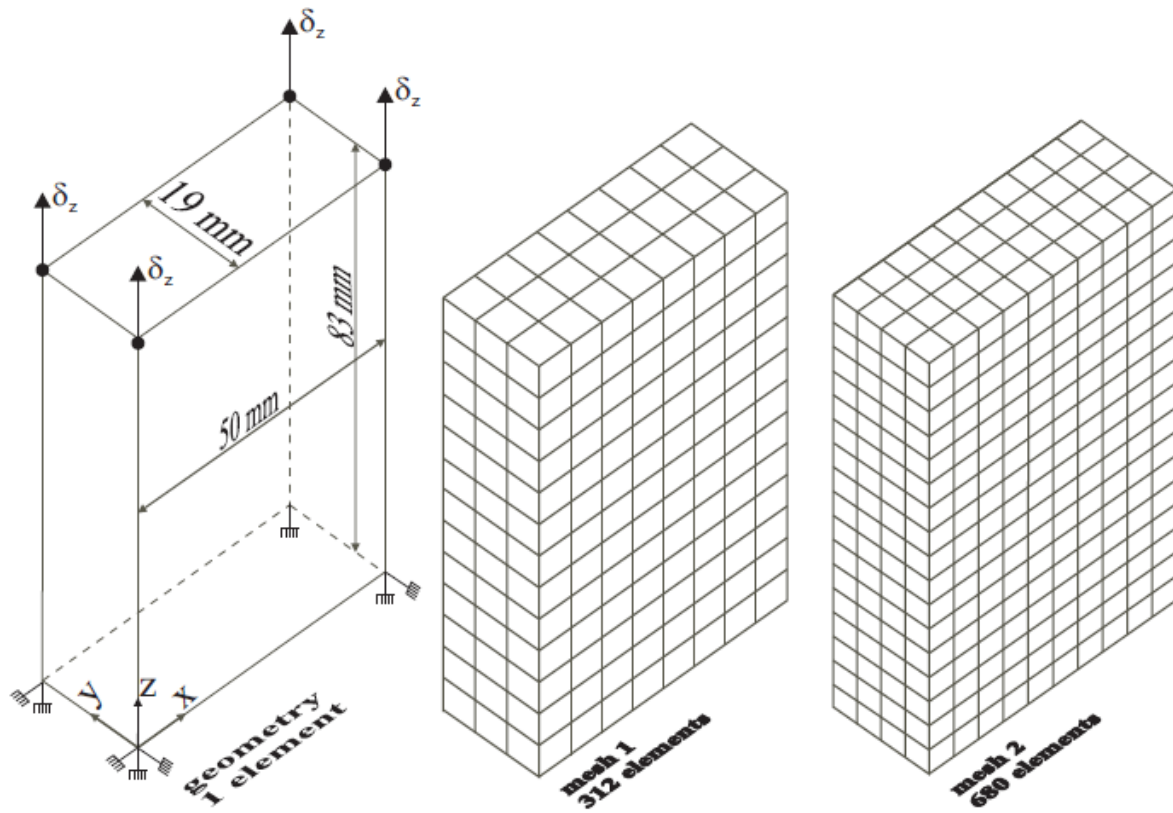
Figure 8. Geometry and mesh for objectivity analysis.
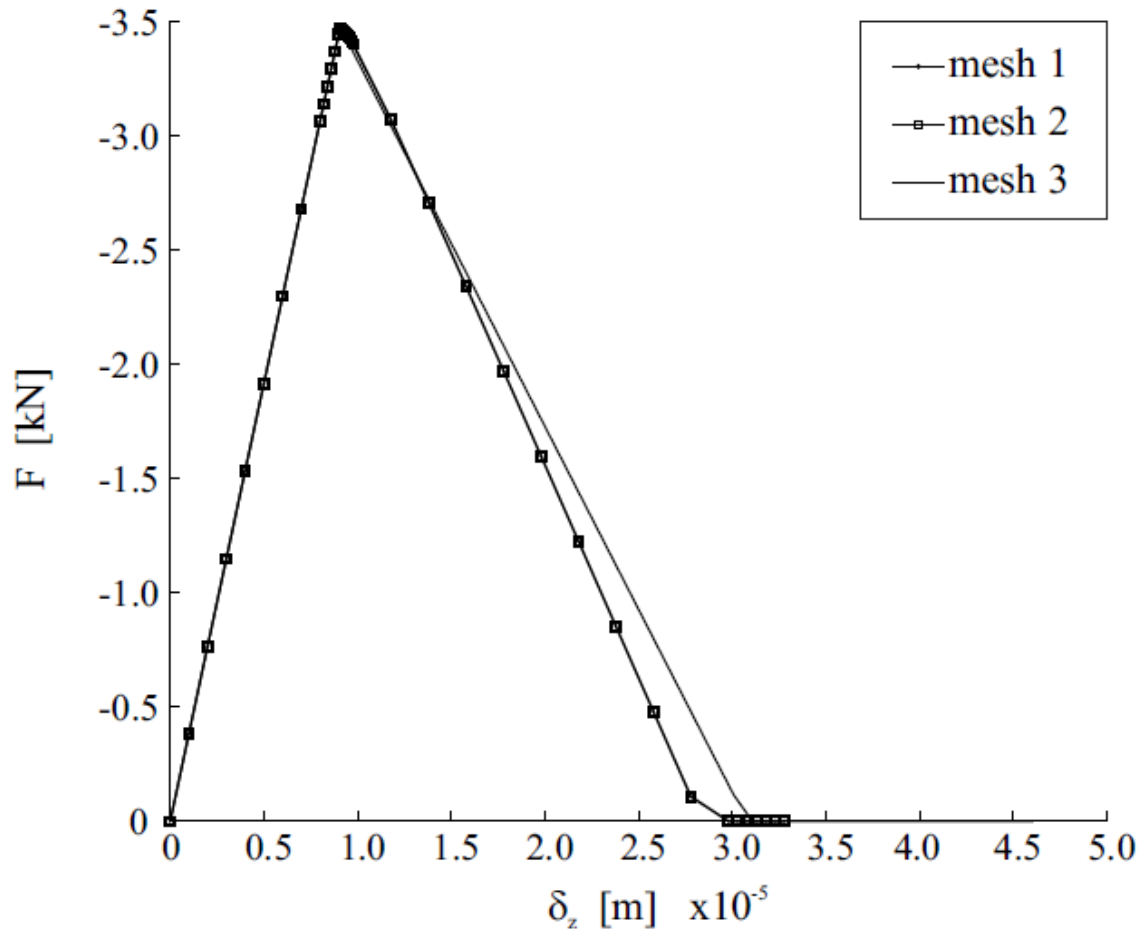
Figure 9. Mesh objectivity. Force-displacement curves for three different meshes. Mesh 1 with 312 elements; mesh 2 with 680 elements and mesh 3 with a single element.
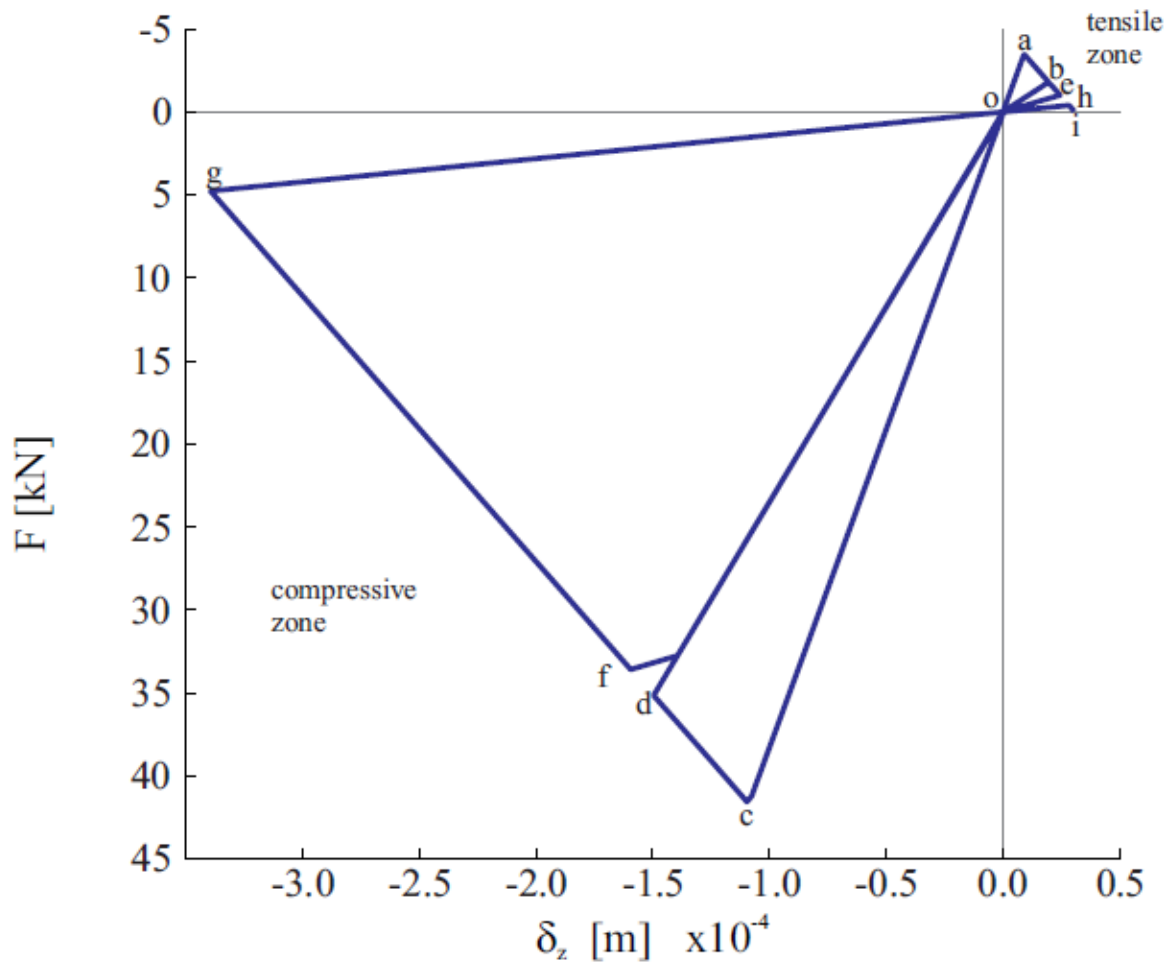
Figure 10. Force displacement curve for reversible loads. The increasing load in segments (o-d) and (o-f) are different, due to the discontinuity between points d and f.
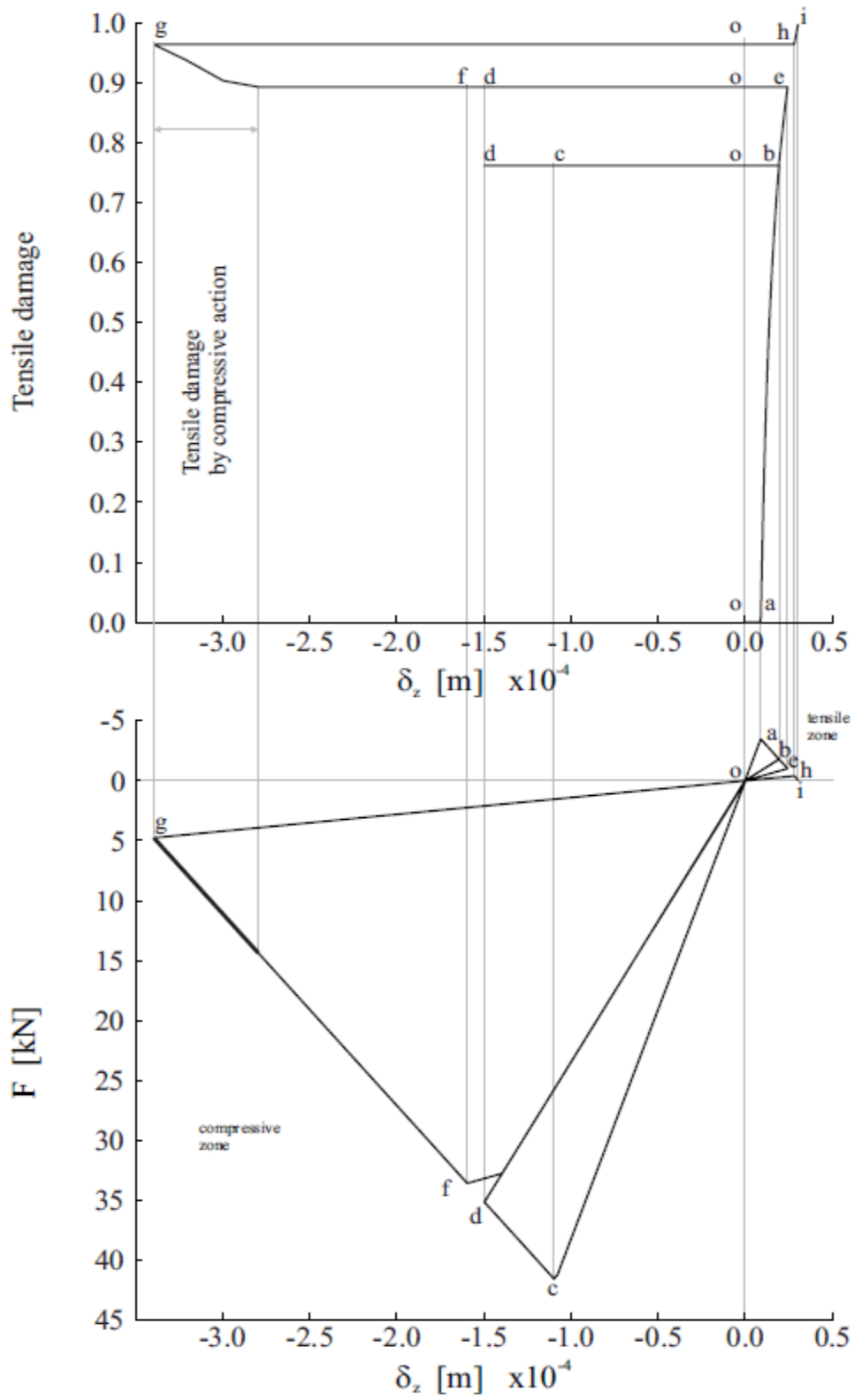
Figure 11. Tensile damage evolution.
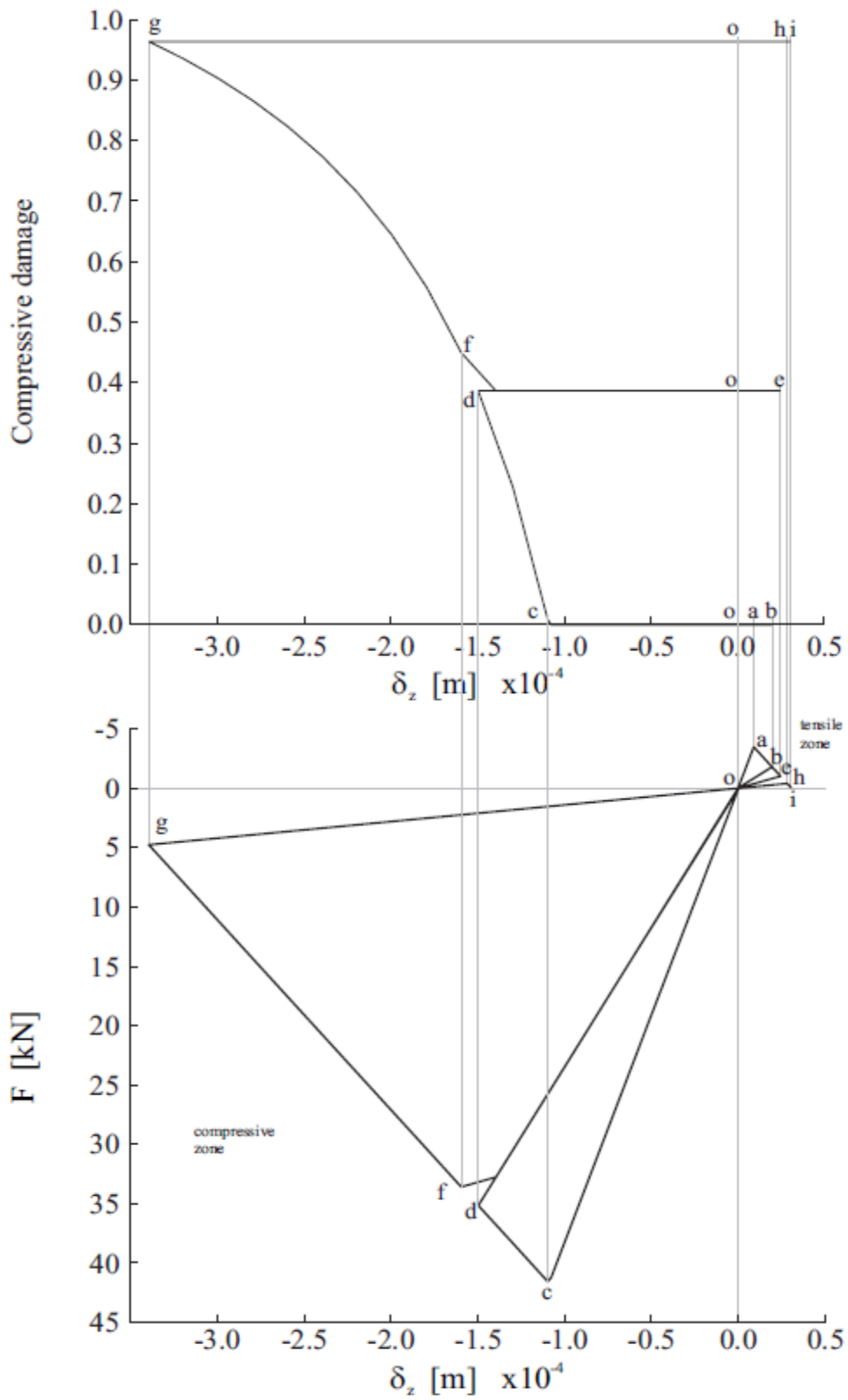
Figure 12. Compressive damage evolution.
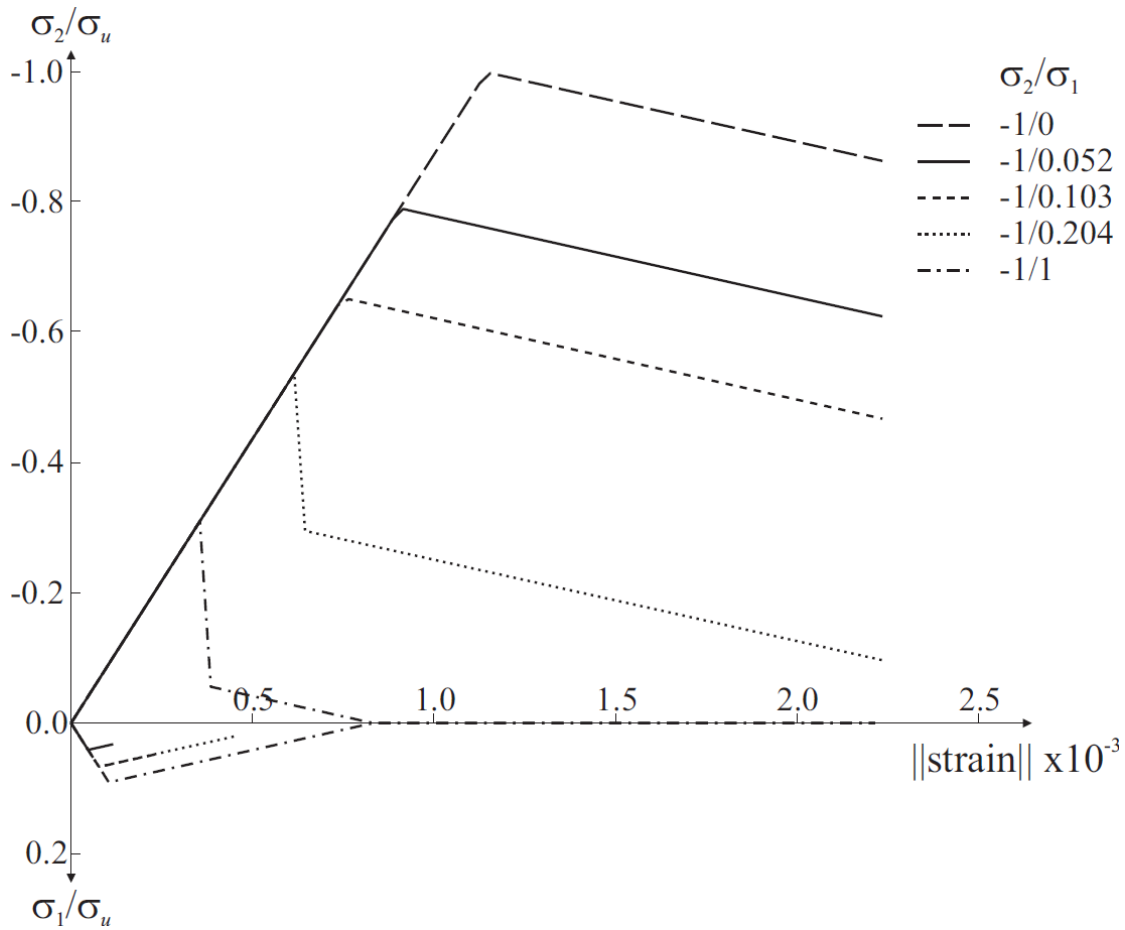
Figure 13. Stress-strain curves for bi-axial loads.
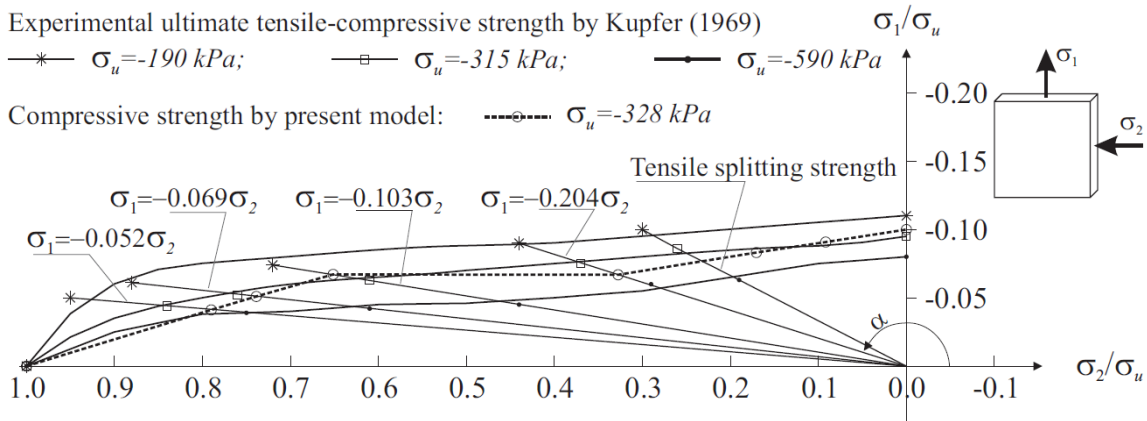
Figure 14. Shear behavior. Experimental ultimate compressive strength by Kupfer et al. 1969: $s_u = -19,0$ MPa; $s_u = -31,5$ MPa; $s_u = -59,0$ MPa.
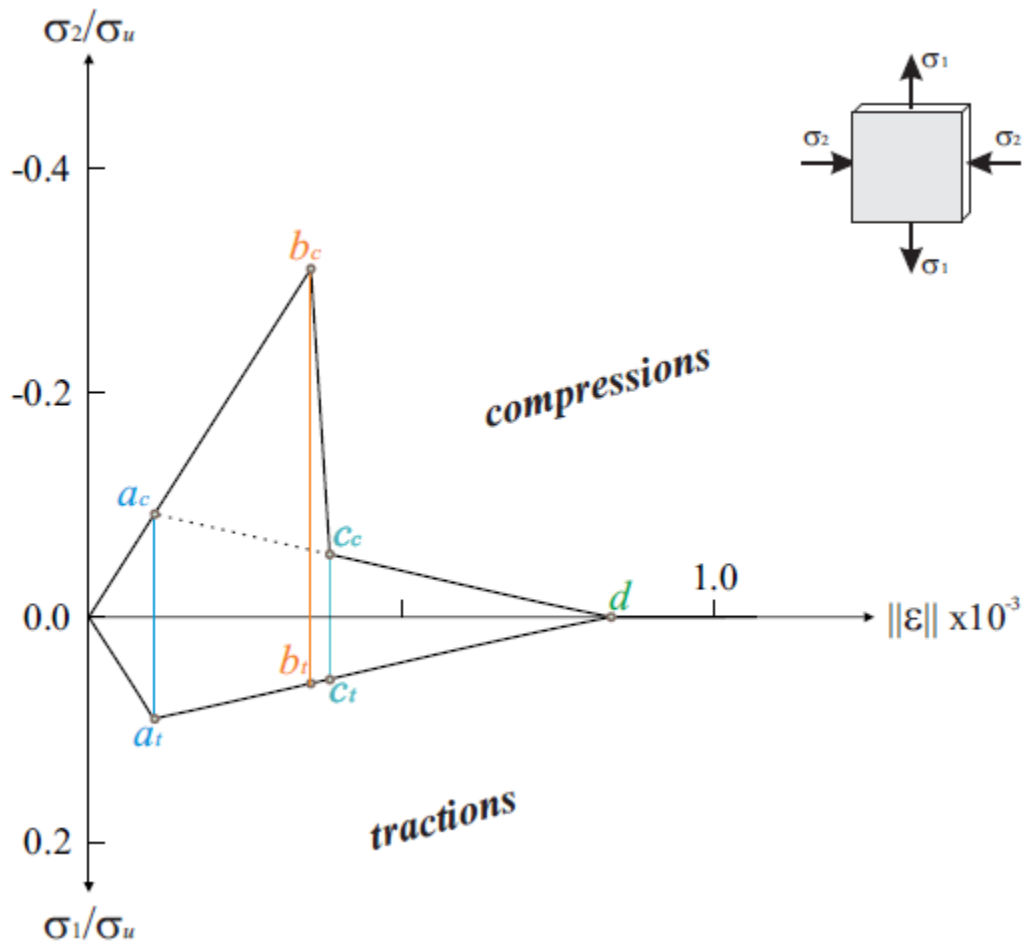
Figure 15. Pure shear behavior.
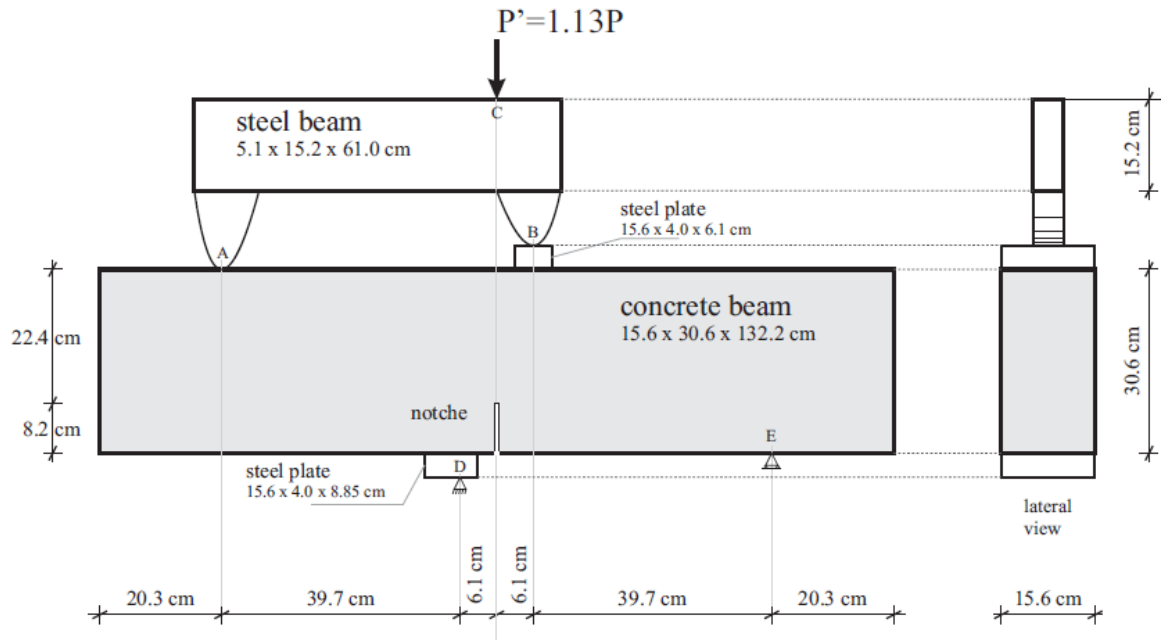
Figure 16. Geometry of concrete beam of Arrea and Ingraffea (1982). Reproduced from Oller (1988).
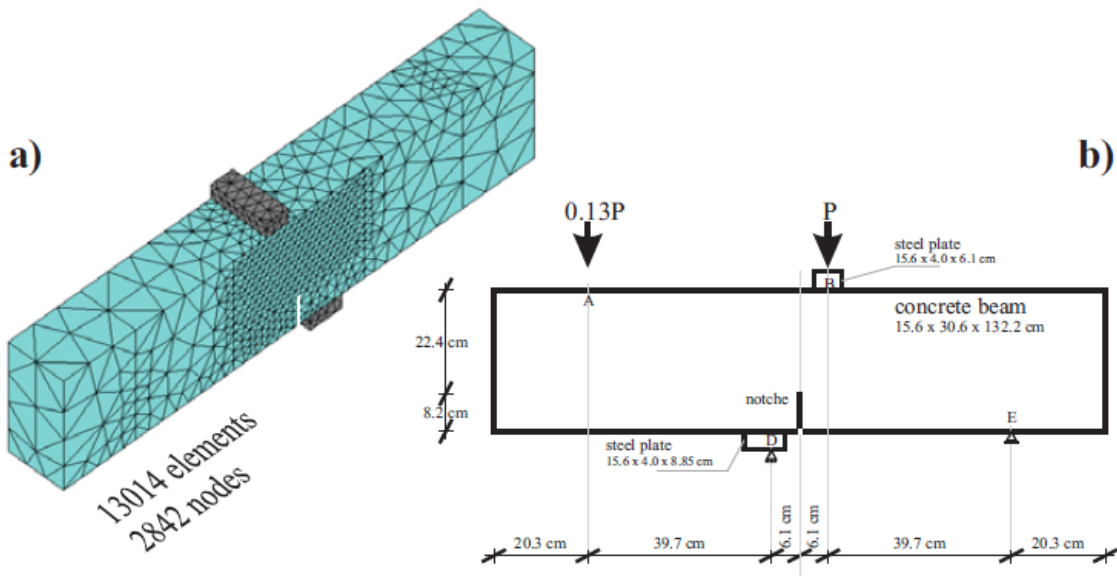
Figure 17. a) Finite element mesh. b) Load and support conditions.
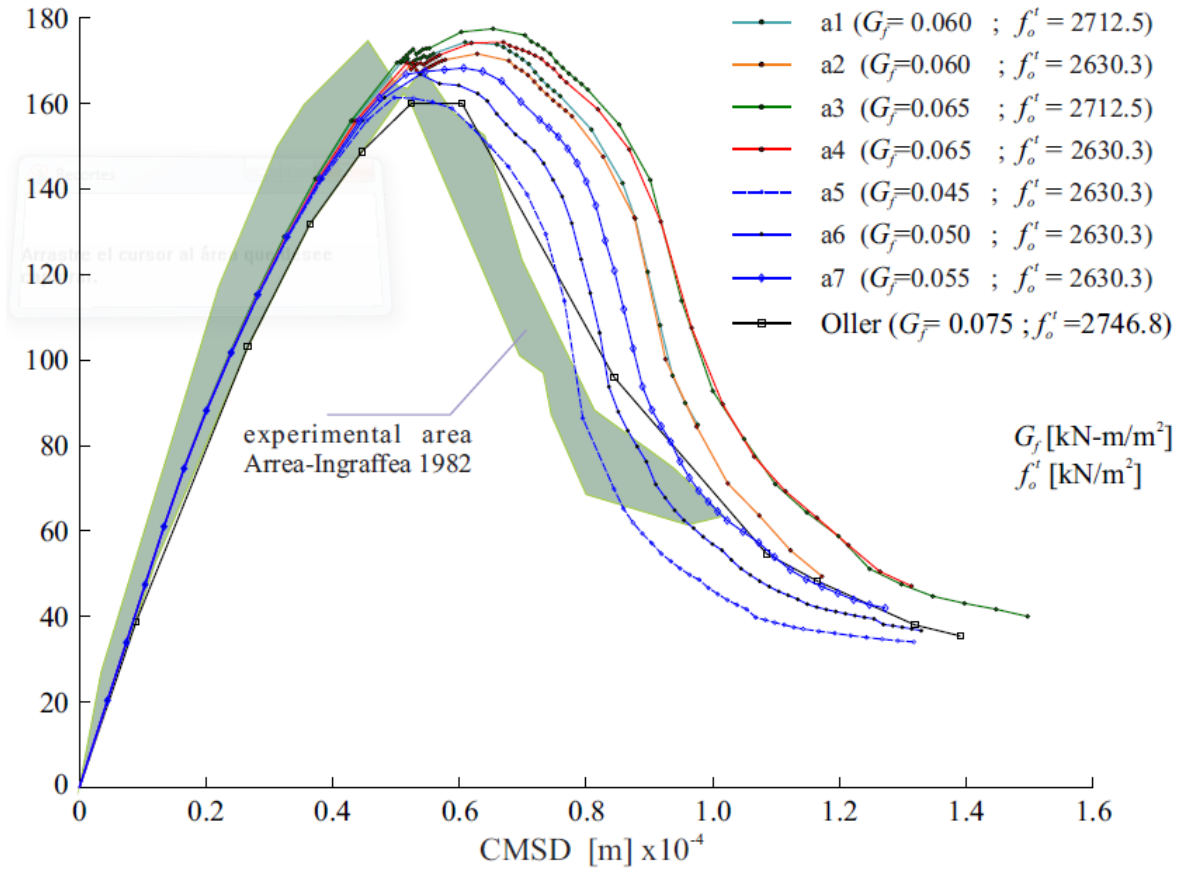
Figure 18. Total vertical reaction force P' vs CMSD curve for series B. Numerical results compared Oller's results (Oller 1988).
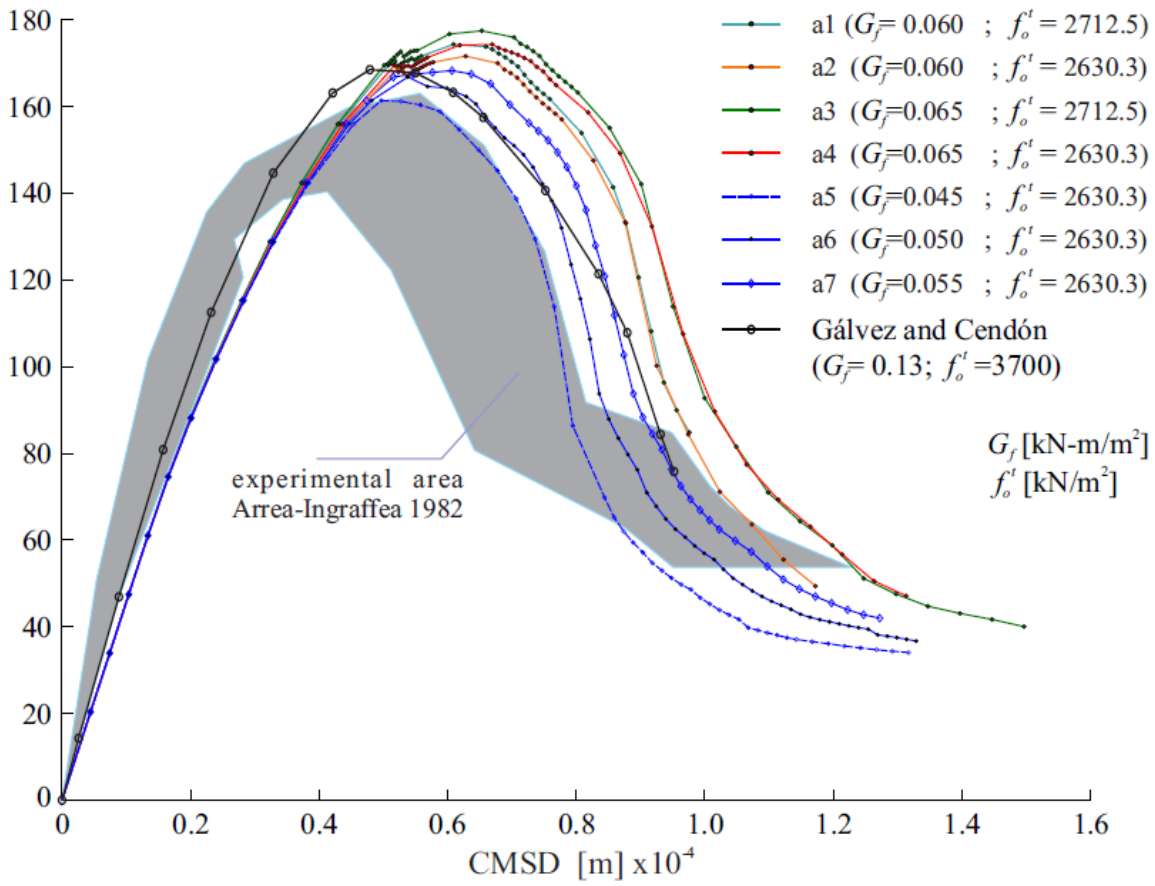
Figure 19. Total vertical reaction force P' vs CMSD curve for series C. Numerical results compared with Gálvez and Cendón's results (2002).
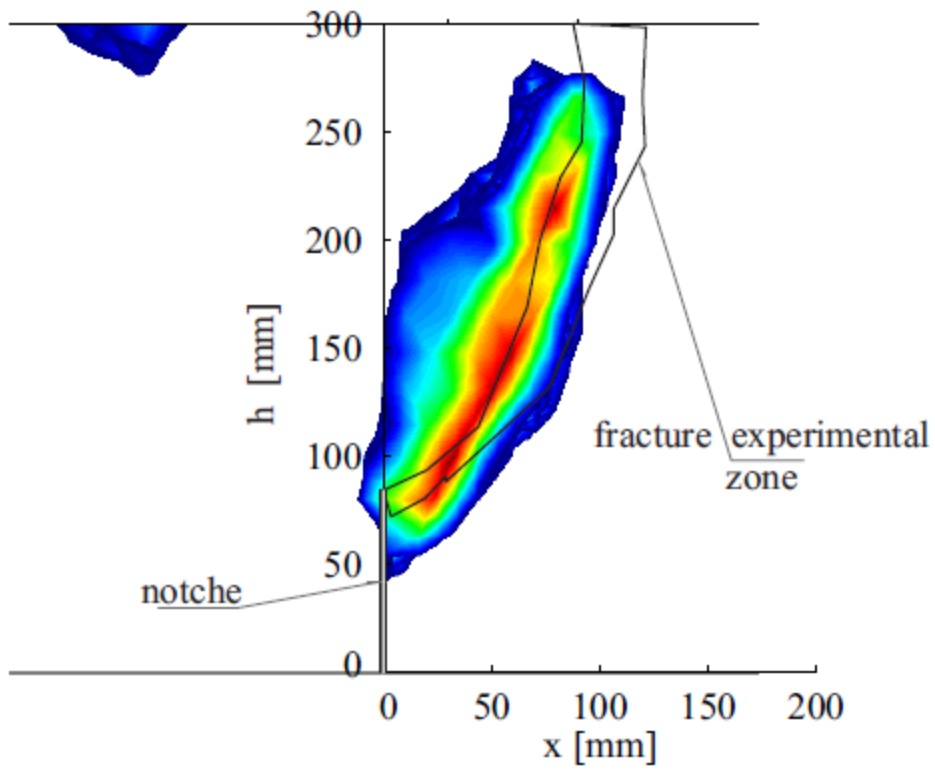
Figure 20. Tensile damage variable in step load 63 overlapped with the experimental cracking pattern.
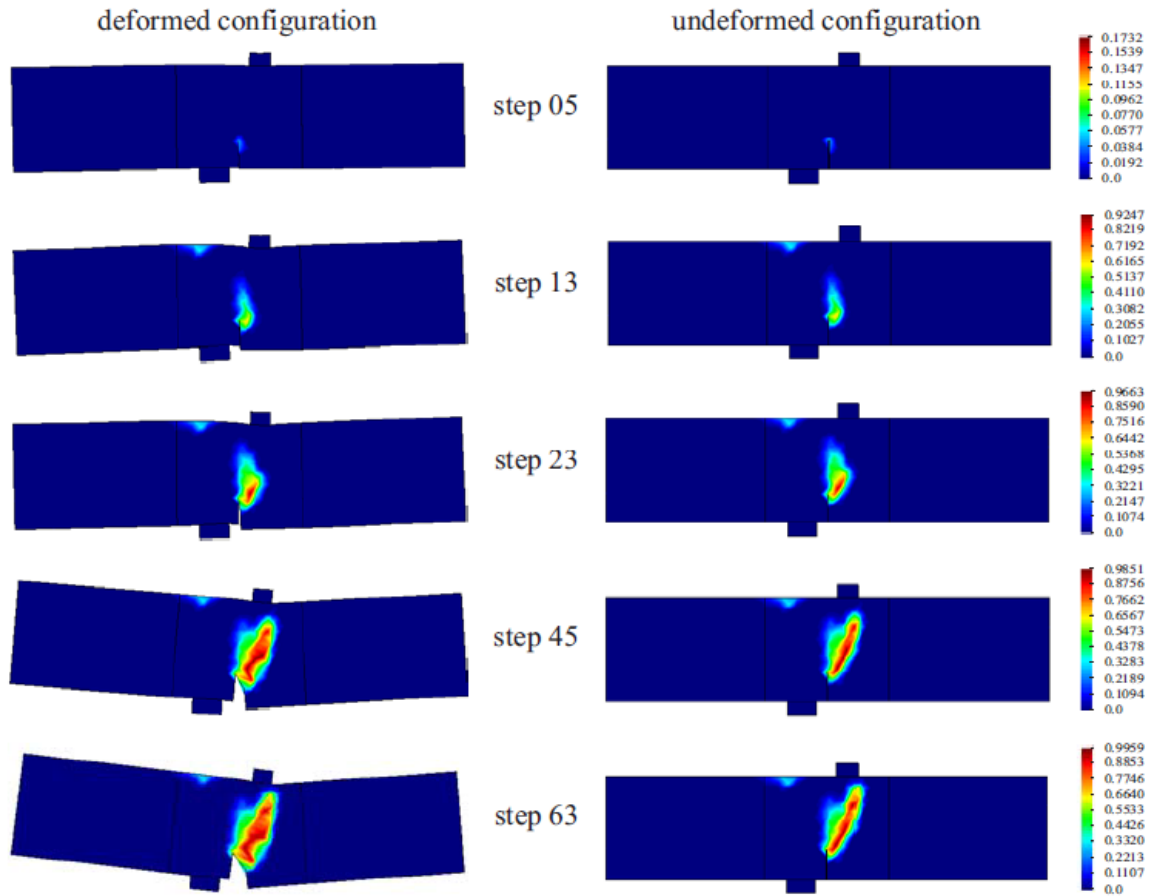
Figure 21. Tensile damage variable evolution. Undeformed and 200 times deformed configurations. Tensile strength of concrete 2630 kPa; compressive strength of concrete 43400 kPa; Ro=16.5; Fracture energy of concrete 0.050 kN-m/m^2.
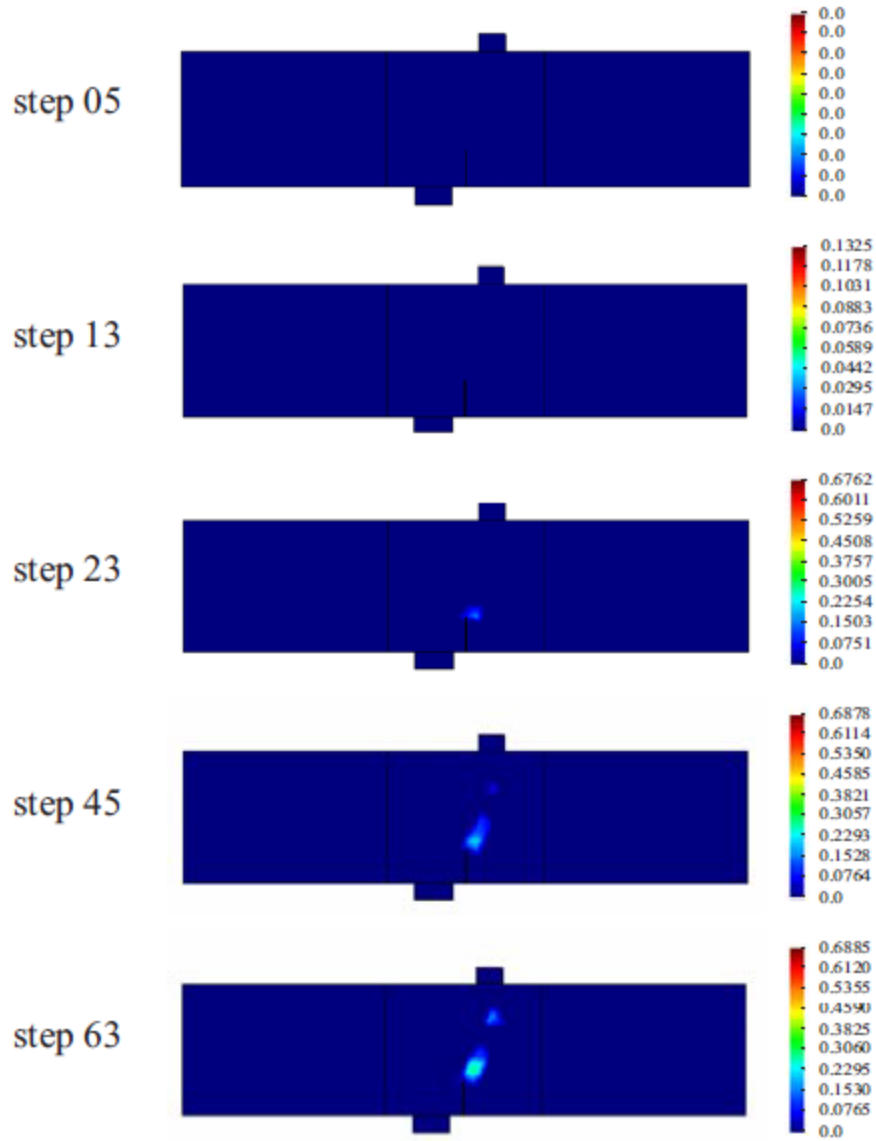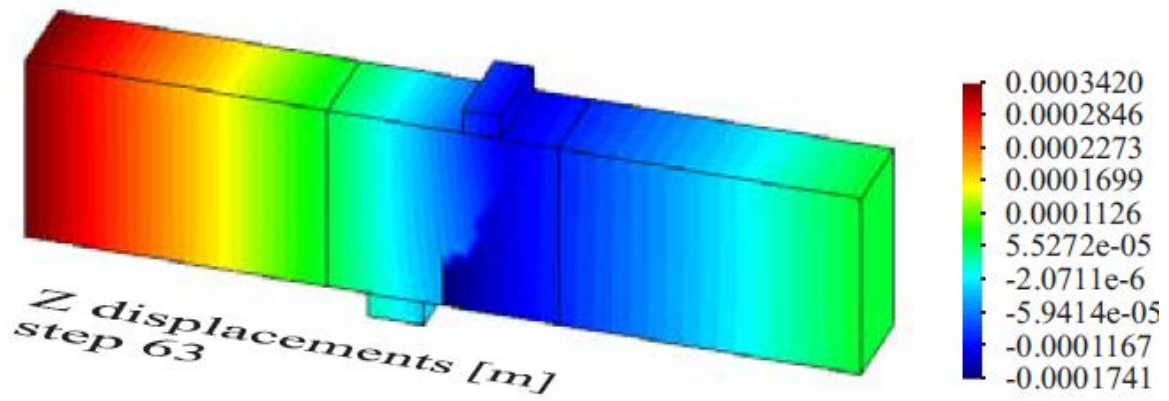
Figure 22. Compressive damage variable evolution. Undeformed configuration. Tensile strength of concrete 2630 kPa; compressive strength of concrete 43400 kPa; Ro=16.5; Fracture energy of concrete 0.050 kN-m/m^2.
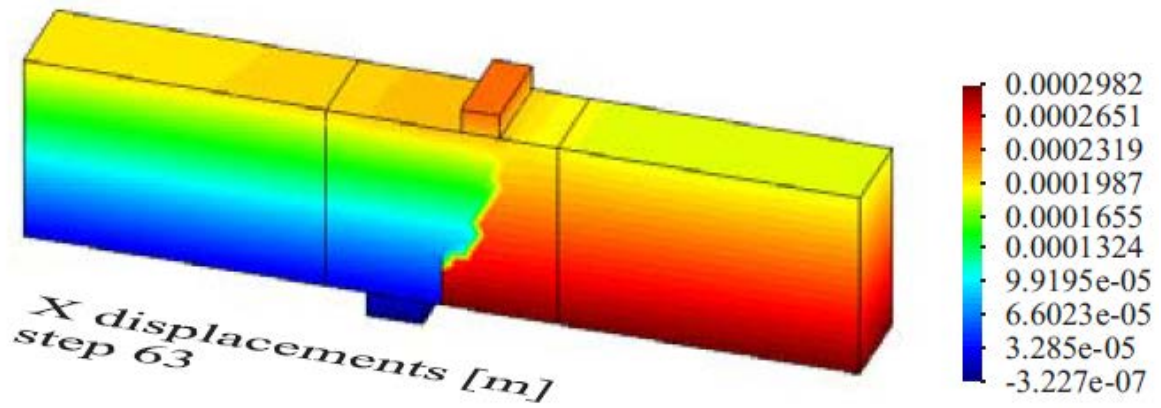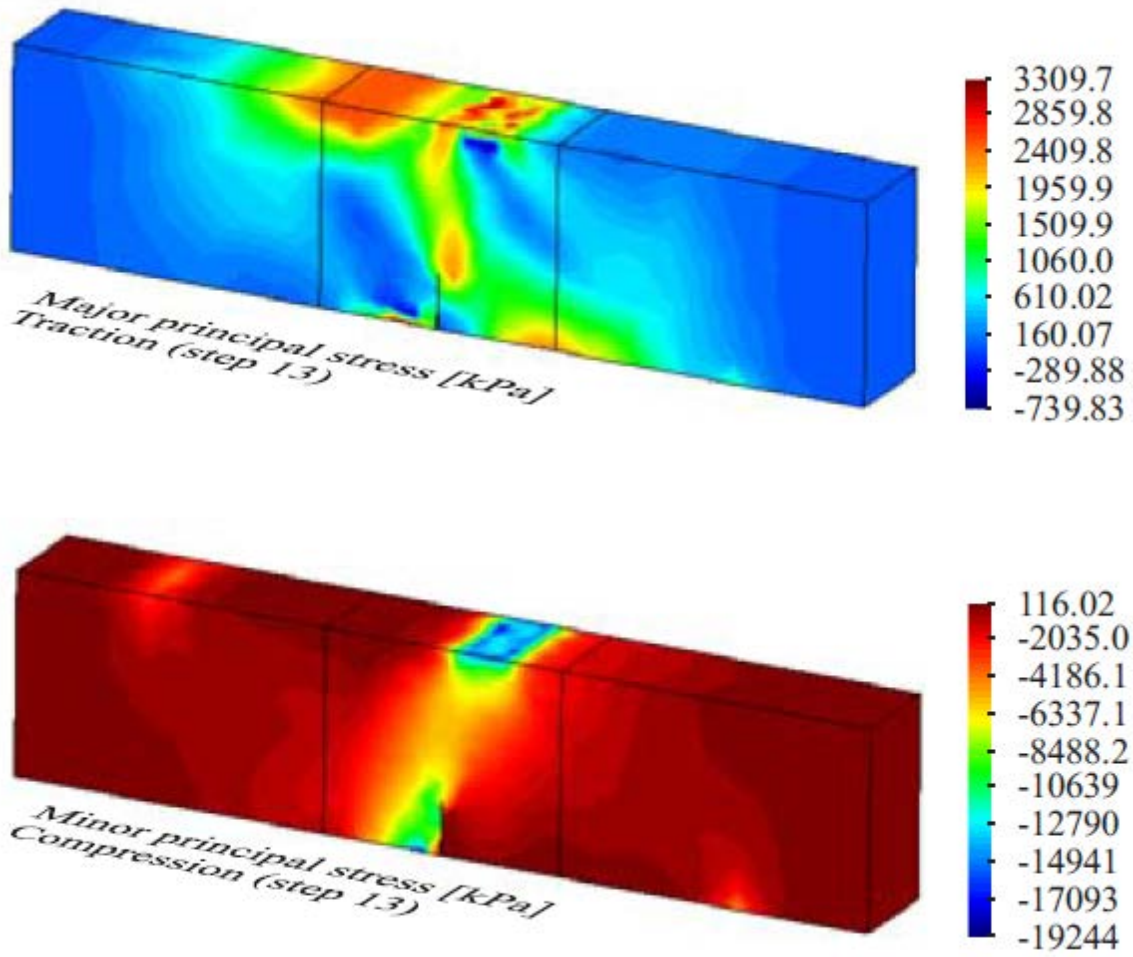
Figure 23. Displacements. Load step 63.

Figure 24. Maximum principal stress (compression) and minimum principal stress (tension) in step load 13.

Table 1. Mechanical properties obtained from Gopalaratnam and Shah (Gopalaratnam and Shah 1985).

Properties	Values
Fracture energy G_f [kN/m]	0.0564
Elasticity modulus x10^6 [kN/m^2]	33.469
Ultimate strength σ_p^t [kN/m^2]	3662.1
Strain ε_p^t x10^{-6} in σ_p^t	120
Damage strength $\sigma_o^t = 0.4\sigma_p^t$ [kN/m^2]	1464.8

Table 2. Calibration of the model with tensile axial load, parameters and results.

Dissipation law	Linear	Hyperbolic	Exponential of Mazars
Parameters	Le=0.083	A1=2.24; A2=0.20; q=0.30	A^+=0.92; B^+= 2.0
Type of dissipation	linear	hyperbolic	exponential
Total energy dissipated Wf [kN-m]. Figure 5	5.359e-5	4.384e-5	4.146e-5
Energy dissipated per unit area. G_f [kN-m/m^2]. Figure 6	0.0564	0.0462	0.0436
Energy dissipated per unit volume. g_f [kN/m^2]. Figure 7	0.6797	0.5560	0.5259

Table 3. Values of the mechanical properties.

Curve	a1	a2	a3	a4	a5	a6	a7
G_f [kN-m/m^2]	0.060	0.060	0.065	0.065	0.045	0.050	0.055
$R_0 = f_o^c / f_o^t$	16.0	16.5	16.0	16.5	16.5	16.5	16.5
f_o^t [kN/m^2]	2712.5	2630.3	2712.5	2630.3	2630.3	2630.3	2630.3